



UNIVERSITY OF GOTHENBURG
SCHOOL OF BUSINESS, ECONOMICS AND LAW

Dynamic Weighting Methods in Portfolio Construction: A Hidden Markov Model Approach

Rasmus Olofsson & Sebastian Wikholm

Master Thesis

Masters of Science in Finance

Marcin Zamojski

(Supervisor)

Graduate School

June 20, 2024

Abstract

This paper explores the application of dynamic portfolio weighting strategies through the integration of Hidden Markov Models with risk parity and equal weighting techniques. Using the concept of market regimes, this study identifies distinct economic conditions based on inflation and growth metrics and develops an investment strategy that adjusts asset allocation conditioned on the macroeconomic climate. The paper contributes to the existing literature by creating a hybrid model that navigates through economic cycles with the goal of improving precision in asset allocation, portfolio diversification, and portfolio resilience. The results underline the Hidden Markov Model's capability to identify market regime shifts based on macroeconomic data and yields positive outcomes in the application of estimated state probabilities as a weighting scheme in a dynamic regime-based investment strategy. The integration of a Hidden Markov Model in the Risk Parity framework, creating the papers hybrid model, improved the portfolio performance, resulted in a higher risk adjusted return and significantly lower drawdowns during the out-of-sample period, compared to the standalone risk-parity portfolios and other portfolios used in the study.

Keywords: Dynamic weighting, State-dependent weighting, Hidden Markov Models (HMM), Market Regimes, Risk Parity, Regime-Switching Models, Portfolio Construction

Acknowledgments

We would like to express our sincere gratitude towards our supervisor, Marcin Zamojski, whose valuable support and input have been crucial during the entire process of this project and the creation of this paper. Without his great commitment and dedication, this paper and the development of the applied strategies would not have been possible. We would also like to thank Erik Hansén at NeuroQuant, not only for highlighting the inspirational work of Ray Dalio and Bridgewater, but also for being our inspiration behind the development of a dynamic, market regime-based strategy.

Contents

1	Introduction	1
2	Literature Review	4
2.1	Market Regimes	4
2.1.1	Economic Cycles and Asset Returns	5
2.1.2	Market Regimes and Asset Allocation	6
2.2	Hidden Markov Model	7
2.2.1	HMM for Dynamic Portfolio Construction	8
2.3	Static Portfolio Weighting	9
2.3.1	Risk Parity	9
2.3.2	Equally Weighted Portfolio	11
3	Methodology	13
3.1	Macroeconomic Environment	13
3.2	Hidden Markov Models	13
3.2.1	Forward-Backward Procedure	15
3.2.2	Viterbi Algorithm	16
3.2.3	Baum-Welch Algorithm	17
3.2.4	Gaussian HMM	19
3.3	Fitting of Hidden Markov Models	20
3.3.1	Model Evaluation	21
3.4	Portfolio Construction	22
3.4.1	Equally Weighted Portfolio Construction	23
3.4.2	Risk Parity Portfolio Construction	23
3.4.3	Dual Layered Static Portfolios	24
3.4.4	Hidden Markov Model for Dynamic Weighting	25
3.4.5	Smoothed Dynamic Weights	25
3.5	Performance Measures	26
4	Monte Carlo	28
4.1	Sample Generation	28

4.2	Monte Carlo Results	29
5	Data	32
5.1	Sample Split	34
6	Empirical Results	36
6.1	HMM results	36
6.2	Equal Weighted Portfolio Evaluation	39
6.3	Risk Parity Portfolio Evaluation	41
6.4	Transaction Costs	45
6.5	Factor Performance Analysis	46
7	Conclusions	48
	References	50
A	ETF Factor Regression	54
B	Returns and drawdowns adjusted for transaction costs	55

1 Introduction

In recent times, the global economy has witnessed a notable increase in inflation rates and a rapid increase in interest rates, leading to adverse impacts on the US equity market, among other markets. This period has been characterized not only by declining stock prices and reduced equity returns but also by increased volatility, making investor portfolios more uncertain and riskier (Huang et al., 2016). Traditionally, bonds are considered a 'safe haven' investment compared to equities, especially during market downturns (Chung Baek, 2021). However, the recent rapid and sharp interest rate hikes by the FED (Reuters, 2022) have worsened the performance and returns of bonds, contrary to their usual role as a refuge during economic turmoil. Several studies indicate that the returns of different asset classes exhibit non-stationarity conditioned on the current economic climate (Ang and Chen, 2002; Cappiello et al., 2006). This study aims to utilize this by creating a state-dependent weighting scheme using a regime switching model that provides robust performance in various economic climates.

The implementation of macroeconomic-dependent investment strategies in this paper is heavily dependent on the concept of market regimes. Ray Dalio, the founder of Bridgewater Associates, one of the largest hedge funds globally, has been a pioneer in this area with the development of the 'All Weather Strategy' (Bridgewater, 2012). The state-dependent strategy implemented in this paper is strongly based on the fact that financial markets experience various seasons or regimes influenced by economic growth and inflation. Hence, identifying macroeconomic climates in which different assets are benefited becomes crucial. Dalio, along with subsequent developers, identifies four primary market regimes based on combinations of high and low growth and inflation (Bridgewater, 2009; Shahidi and Lee, 2014).

A crucial part of the implementation of the Bridgewater Associates framework is the inclusion of a wider set of asset classes along with an allocation method called risk parity (Bridgewater, 2009). The inclusion of less traditional assets in the portfolio composition, such as Treasury Inflation Protected Securities (TIPS), has been shown to be a valuable component in any diversified portfolio, as they provide a hedge against inflation and mitigate some of the negative effects of declines in both the equity and bond market (Laatsch and Klein, 2003). The risk-parity method seeks to equalize the risk contribution

across a wider set of asset classes, rather than distributing capital equally among them (Qian, 2011). This approach contrasts with conventional portfolio strategies that typically have a higher allocation to stocks and bonds and aims to decrease portfolio dependency on one asset or market (Prince, 2010).

Developing an investment strategy based on market conditions, an investor can opt for either a static or dynamic method. A static approach, as referenced by Bridgewater (2009) and Shahidi and Lee (2014), entails equal exposure towards all market regimes. Dalio clarifies this approach by noting that due to the unpredictability of future market conditions, it is prudent to always have the portfolio prepared for any scenario (Bridgewater, 2009). In contrast, a dynamic method requires the investor to modify the portfolio allocation in response to varying market conditions over time. According to Dahlquist and Harvey (2001), when economic conditions persist and have a significant impact on asset returns, a dynamic strategy is likely to be more beneficial than a static one. We evaluate the benefits of using a dynamic strategy by constructing both static and dynamic portfolios.

The creation of a dynamic state-dependent investment strategy in this paper employs a regime-switching model similar to previous studies (Kritzman et al., 2012; Nystrup et al., 2018). This paper uses the Hidden Markov Model (HMM) to determine a state-dependent allocation reflecting probabilities of all states, recognizing the most likely prevailing market regime at any given time. HMM are powerful statistical models, adept at examining time series data where the system's states are 'hidden' and only the observable output data are observable (Rabiner, 1989). In the realm of finance, HMMs are commonly utilized to detect hidden patterns in market behavior and forecast regime changes (Kritzman et al., 2012). These models provide investors with a suitable framework to adjust their portfolio allocation based on anticipated economic conditions, thus mitigating risks and improving returns across various market regimes (Kritzman et al., 2012; Liu, 2011; Nystrup et al., 2018).

We examine the relative performance of static and dynamic portfolios. The creation of static and dynamic portfolios is done by building state-optimal portfolios using either an equal weighting scheme or the risk-parity method, which are subsequently combined into an overarching main portfolio.

This paper contributes to the existing literature by integrating HMM and risk parity

into a market-regime-based investment strategy, creating a hybrid strategy that navigates through economic cycles with the goal of improving precision in asset allocation, portfolio diversification, and portfolio resilience. Through model development and empirical tests, this paper evaluates the efficiency of Hidden Markov Models in managing and predicting the dynamics of market changes.

The empirical results of this thesis highlight the viability of incorporating state-dependent weighting schemes to create a dynamic portfolio. Our dynamic strategies demonstrate significant improvements in out-of-sample performance compared to their static counterparts, which are consistent with previous findings (Kritzman et al., 2012; Nystrup et al., 2018; Elliott and Hinz, 2002). Furthermore, the effectiveness of Hidden Markov Models in out-of-sample estimation successfully adjusts portfolio allocation toward more desirable asset classes, reinforcing previous findings (Kritzman et al., 2012; Liu, 2011; Nystrup et al., 2018).

In summary, this paper demonstrates that a dynamic investment strategy that incorporates HMM and risk parity can significantly improve portfolio performance in varying macroeconomic climates. However, the complexity and requirement for careful implementation underscore the challenges that must be addressed before practical use, and to overcome these, the strategy requires additional refinement.

2 Literature Review

In this section, we introduce concepts and previous findings with a focus on market regimes and macroeconomic factors influencing asset return, Hidden Markov models and their usage within portfolio construction and regime estimation, and lastly two different weighting methods.

2.1 Market Regimes

Understanding the complex interaction between macroeconomic factors and asset returns is crucial to create robust investment strategies. This interplay is dynamic, making it essential for investors to account for economic indicators when planning investments.

Flannery and Protopapadakis (2002) demonstrates how macroeconomic factors have a substantial influence on aggregate stock returns. The study highlights variables such as inflation, money supply, employment reports and housing starts as key drivers affecting both the level and volatility of returns. The relationship between macroeconomic factors and returns is not limited to equities. For example Ang and Chen (2002); Cappiello et al. (2006) show how returns and volatility for various asset classes are affected by macroeconomic dependencies such as industrial production and GDP growth. Their findings indicate that the connection between economic growth metrics and asset returns is complex and shows asymmetrical characteristics. In other words, the influence of macroeconomic fluctuations on asset returns can differ depending on whether the economy is expanding or contracting. Furthermore, shifting market conditions also creates asymmetric correlations among different assets (Chua et al., 2009). Asymmetry in the correlation structure among assets suggest that traditional diversification strategies provides limited upside during periods of turbulence of significant macroeconomic shifts.

"When looking back through history, there is one thing we can see with absolute certainty: every investment has an ideal environment in which it flourishes. In other words, there's a season for everything. I know that there are good and bad environments for all asset classes. (...) But the key thing is that there are basically four economic environments. There are two main drivers of asset class returns: inflation and growth." - Ray Dalio (Council on Foreign

Relations, 2012)

Bridgewater Associates proposes that their All Weather investment strategy not only endures but also prospers in any economic condition, regardless of whether it is inflationary or deflationary or whether it is during periods of economic growth or decline. The strategy relies on a statistical analysis of how inflation and economic growth uniquely impact asset returns, and prescribes a disciplined risk parity approach to asset allocation.

2.1.1 Economic Cycles and Asset Returns

Bridgewater (2012) and Shahidi and Lee (2014) emphasize that economic cycles, consisting of changes in economic growth and inflation, are fundamental drivers of asset class returns. They divide the economic environment exclusively by the two dynamic and interrelated factors:

Economic Growth: Shifts in economic growth significantly affect the investment returns. Typically, robust economic growth strengthens equities as businesses thrive, which drives earnings and stock prices. In contrast, periods of weak or declining growth increase the appeal of less risky assets such as treasuries, which tend to offer safety and a fixed return when riskier assets like stocks are unattractive (Masoud, 2013; Aleksandar Andonov and Lehnert, 2010).

Inflation: Trends in inflation play a crucial role in defining the real earnings and the ability to preserve wealth of various asset classes. Rising inflation generally benefits tangible assets such as commodities and real estate, which can act as hedges against deterioration of monetary value. Meanwhile, during deflationary periods when prices decline, bonds tend to perform, particularly long-term government securities, since the real value of their fixed returns increases (Fuertes Mendoza, 2023; Magnus Andersson and Vähämaa, 2008).

The dynamic interaction between high and low economic growth and inflation can effectively be divided into four different categorized market regimes, each representing a unique macroeconomic environment that has different impacts on asset returns. By mapping these two critical factors into a two-dimensional space, we identify four regimes (Figure 1): high growth with high inflation, high growth with low inflation, low growth with high inflation and low growth with low inflation. Each of these market regimes requires specific strategic asset allocations to optimize returns and mitigate risks. This

two-dimensional space framework not only simplifies the complex dynamics among the economic conditions, but also enables better portfolio management by tailoring asset selection to the prevailing market regime (Shahidi and Lee, 2014). Through such a structured approach, investors will be able to systematically adjust their portfolios to capitalize on the opportunities and hedge against the downturns presented by each distinct market regime.

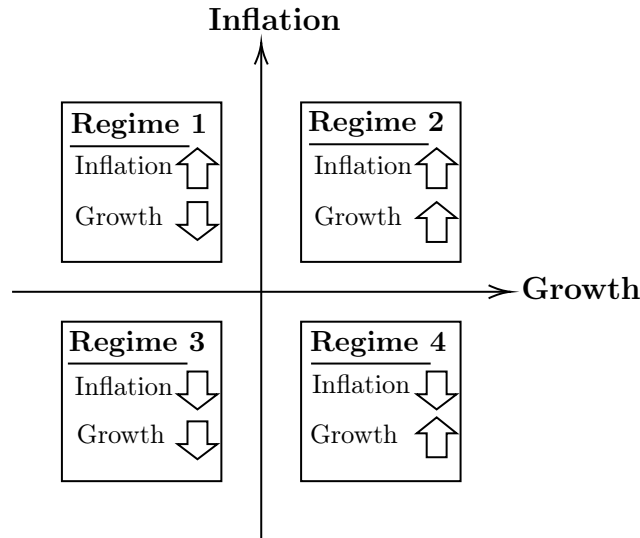


Figure 1: Breakdown of each market regimes characteristics in terms of growth and inflation

2.1.2 Market Regimes and Asset Allocation

Bridgewater (2012) and Shahidi and Lee (2014) propose that tailoring the portfolio to the two-dimensional space framework seen in Figure 1 by incorporating assets that perform well in each scenario allows investors to mitigate the major risks associated with each market regime. Adapting the portfolio to the two-dimensional framework requires including assets that benefit from the two dynamic factors of economic growth and inflation during both upward and downward trends:

- **Rising Growth:** A market regime characterized by increasing growth indicates an optimal environment for risky assets such as equities and commodities. These assets typically capitalize on an expanding economy as consumer spending increases and corporate profits grow (Masoud, 2013).

- **Falling Growth:** In a regime with falling economic growth, defensive assets such as governmental treasuries and Treasury inflation-protected securities (TIPS) are more favorable. These assets offer stable returns and are less correlated with the outcome of the broader economy (Aleksandar Andonov and Lehnert, 2010).
- **Rising Inflation:** During periods of rising inflation, the portfolio should consist of a larger portion of assets that maintain real value, such as commodities and TIPS. These assets can protect against the loss of purchasing power that is generally associated with inflation (Fuertes Mendoza, 2023).
- **Falling Inflation:** In environments where inflation is falling, traditional assets such as stocks and bonds perform well. Bonds increase in value as the real value of future cash flows increases, and equities are favored by the lower interest rates that typically accompany lower inflation (Magnus Andersson and Vähämaa, 2008).

The essence of these authors' arguments is that no single asset class consistently outperforms in all market regimes. Hence, a diversified portfolio comprising various asset classes is essential to reduce risks and capitalize on opportunities in different market scenarios. Shahidi and Lee (2014) advocates for a balanced static asset allocation strategy, inspired by Ray Dalio's All Weather approach, which seeks to deliver stable returns in both favorable and unfavorable economic periods. In contrast, in this paper, we employ a dynamic strategy with state-dependent weighting to adjust portfolio allocation based on evolving market conditions.

2.2 Hidden Markov Model

To identify the current market regime and subsequently develop our state-dependent portfolios, we utilize a Hidden Markov Model (HMM). An HMM is a statistical framework that models systems in which observations or events are dependent on hidden or latent states. HMMs presume a finite set of hidden states that are not directly observable but transition according to a Markov process, where the likelihood of moving to the next state depends only on the current state (Rabiner, 1989). In the realm of finance, HMMs are commonly used for tasks such as detecting market trends and optimizing portfolios based on regime-specific events, making them suitable for identifying market regimes (Çanakoglu

and Özekici, 2011; Nystrup et al., 2018). By linking these hidden states to bull and bear trends, the detection of the market regime allows investors to adjust their strategies in response to expected market shifts (Nystrup et al., 2018).

2.2.1 HMM for Dynamic Portfolio Construction

Considering the non-stationarity in asset returns (Ang and Chen, 2002; Cappiello et al., 2006), the potential advantages of adjusting the portfolio based on regime-specific estimates might be preferable. For example, an increased exposure towards risky asset during periods of economic ambiguity has been shown to be beneficiary, regardless of investment horizon (Liu, 2011).

Kritzman et al. (2012) explores how HMM can be dynamically incorporated in portfolio construction to adjust allocation based on the relative likelihood of a given market regime. By identifying regimes for variables like inflation and economic growth, they demonstrate that dynamic regime-switching allocation significantly outperforms unconditional static alternatives. Using regime switching models like the HMM to predict economic regimes enables investors to re-calibrate their portfolio favorably towards the prevailing trends in the market. By identifying characteristics of assets that are positively or negatively impacted by the trends of macro-variables in a given regime the portfolio is easily tilted to a favorable position. Nguyen and Nguyen (2015) demonstrates the effectiveness of tilting the portfolio based on factors positively rewarded in a given macroeconomic environment. Examining the traits of stocks in the S&P 500 index that were favorably influenced by the current market regime, Nguyen and Nguyen (2015) dynamically adjusts the portfolio according to the predicted market regimes. The resulting portfolio generated superior performance in not only total returns but also when adjusted for risk, highlighting the robustness and reliability of the strategy.

The application of Hidden Markov Models (HMM) in portfolio construction has gained attention because of their capability to represent complex, dynamic financial systems where market states are not directly observable. HMMs are especially useful for predicting regime changes and adjusting portfolio strategies accordingly. For example, Hua and Wang (2014) combine HMM with a regime switching framework to optimize investment strategies, showing that HMM can adeptly manage the dynamic nature of financial markets. Similarly, Çanakoglu and Özekici (2011) employ HMM for portfolio selection

under imperfect information, showing that even with partially observable market states, HMM can still provide solid investment strategies. Further studies emphasize the flexibility of HMM in portfolio optimization, increasing portfolio performance through recursive algorithms (Elliott and Hinz, 2002).

The capability of a dynamic investment strategy that employs a regime switching model to reduce downside risk and capitalize on positive market trends by identifying market changes is emphasized by Nystrup et al. (2018). The possibility of proactive reallocation is the essence of what enables dynamic regime-switching investment strategies to generate superior performance relative to traditional and static strategies (Nystrup et al., 2018; Liu, 2011). Kim et al. (2019) expands on the idea of proactive allocation via the usage of HMM by showing how changing market conditions can be mirrored and therefore counteracted.

Although numerous studies suggest a beneficial effect of adopting regime-switching investment strategies, the evidence is not entirely favorable. Dacco and Satchell (1999) emphasize a discrepancy between the promising in-sample performance of regime-switching models and their often disappointing out-of-sample forecasting ability. They point out that the inherent challenge of accurately predicting future market regimes significantly underestimates the effectiveness of these models for financial forecasting. This suggests a fundamental limitation of their utility for predictive analysis. The issue is further contrasted with the performance of random-walk models, implying that simpler forecasting methods can sometimes offer comparable predictions without the complexity of regime-switching approaches.

2.3 Static Portfolio Weighting

The static portfolios constructed in this paper relies on creating an equal exposure in terms of risk (risk-parity) or ratio of the portfolio (equal weighting) to each market regime or to all assets within the portfolio.

2.3.1 Risk Parity

Pioneered by Bridgewater Associates through the All-Weather portfolio, the risk-parity framework for portfolio weighting aims to equalize the risk of all assets in the portfolio

(Qian, 2011). When introduced, the framework signified a shift from traditional approaches (Roncalli, 2013). By striving to balance the risk contribution of each asset, i.e., establishing risk parity within the portfolio, the method seeks to achieve a more balanced risk distribution relative to traditional approaches, which can improve portfolio diversification and robustness (Bessler et al., 2021). The performance of conventional methods for asset allocation, such as the 60/40 equity/bond split, is highly dependent on the equity market. Disproportional reliance on equities can result in portfolio correlation with the equity market as high as 95% (Bridgewater, 2012). By incorporating a broader range of asset classes into the portfolio and adjusting the weighting strategy to follow the risk-parity approach, advocates argue that the imbalanced risk distribution and significant reliance on the equity market can be mitigated (Shahidi and Lee, 2014; Qian, 2011; Bridgewater, 2012).

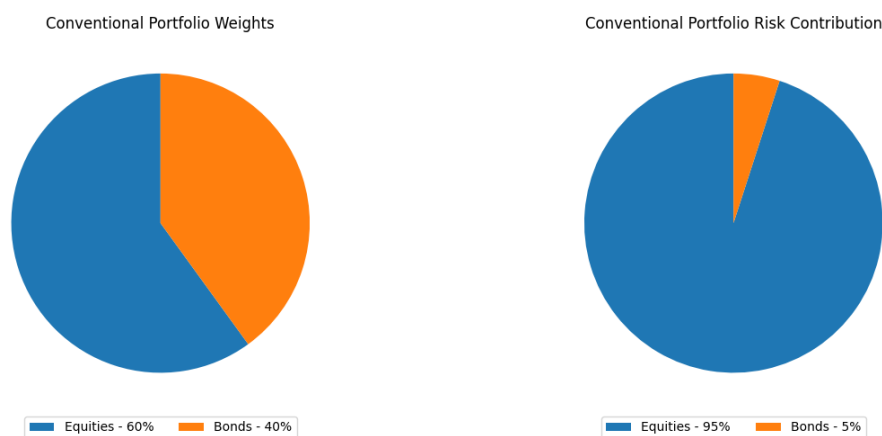


Figure 2: Conventional Portfolio Weights and Risk Contribution

By allocating a smaller portion of the portfolio capital to high-volatility and high-risk assets like equities, and a larger portion to low-volatility assets like bonds, the Risk Parity strategy ensures an equal distribution of risk among the portfolio components. Practically, risk-parity builds on identifying each component's marginal risk contribution and then adjusting the weights such that each portfolio component contributes an equal amount to the total portfolio risk (see Section 3.4.2 for details) (Qian, 2011). This results in a portfolio that avoids excessive reliance on any single type of asset or market (Prince, 2010).

Qian (2011) clarifies the core principles of Risk Parity and underscores the paradigm shift towards a risk-centered allocation framework. Qian (2011) criticizes the conditional

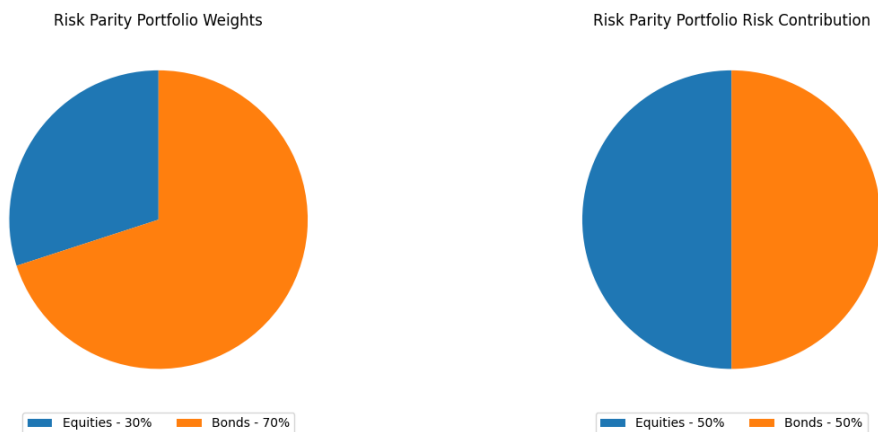


Figure 3: Risk Parity Portfolio Weights and Risk Contribution

equity-centered portfolios for their disproportional risk exposure and favors a model where risk, rather than capital, is the main factor controlling allocation decisions. This approach results in portfolios that are inherently more stable and equipped to handle the fluctuations of market dynamics, offering more consistent performance (Prince, 2010; Qian, 2011).

In addition, Bridgewater’s adaptive strategy framework, especially their provision for a ‘safe portfolio’ during depressive market conditions, illustrates the flexibility of the model and its preventive stance against extreme market downturns (Prince, 2010). This strategic agility confirms the ability of risk-parity to effectively mitigate risks, even during turbulent financial climates.

Among the criticisms of risk-parity, Fabozzi et al. (2021) points out specific challenges that the strategy faces. One of the primary issues is the selection of asset classes to be included in the portfolio. Poor or incorrect selection can lead to sub-optimal diversification and risk management. Additionally, the choice of risk metrics can influence the portfolio performance. They also discuss the decision between active and passive asset selection within each asset class, which can impact risk-adjusted return and diversification benefits.

2.3.2 Equally Weighted Portfolio

To enable the evaluation of the contribution of risk-parity to overall portfolio performance, we construct additional static portfolios using an equally weighted strategy.

The equally weighted diversification framework provides a simple method of spreading portfolio risk by allocating capital equally to each asset in the portfolio (DeMiguel et al., 2009). The addition of monthly re-balancing is shown by Bouchey et al. (2012) to generate

higher returns than a comparable equally weighted buy and hold strategy. Additionally, DeMiguel et al. (2009); Plyakha et al. (2012) provides empirical evidence for the equally weighted strategy generating higher mean returns relative to price- and value weighted portfolios. The increased returns of the equally weighted strategy can be attributed to two main factors. Firstly, it shows an increased exposure to market, size, and value risk factors. Secondly, its higher alpha is due to the monthly re-balancing, which benefits from stock return characteristics such as reversal, idiosyncratic volatility, and lead-lag patterns at the monthly level (Plyakha et al., 2012)

3 Methodology

3.1 Macroeconomic Environment

The breakdown of the interplay between asset returns and the economic cycle opens up several possibilities for portfolio construction, where the current economic climate is a driving force for asset allocation. However, an issue arises in determining the current climate given the untimely reporting of actual macroeconomic data and the precision of the said data. The lag of real growth and inflation data becomes apparent when considering the ex post reporting adjustments, and as such determining the current macroeconomic climate in real time presents a challenge.

3.2 Hidden Markov Models

Hidden Markov Models (HMM) provide a framework for modeling latent processes through observable signals originating from the source (Rabiner, 1989) thus providing a suitable approach to determine the macroeconomic climate in real time. The latent variable in an HMM constitutes a doubly embedded stochastic process, wherein an underlying stochastic process remains unobserved, hence termed as "hidden", and can only be inferred through another set of stochastic processes generating the observed sequence (Rabiner, 1989).

Consider a system capable of occupying a specific state q_t at any given point time within a finite state space $S = \{S_1, S_2, S_3, S_4\}$ (as shown in Figure 4). Each state is associated with a distinct set of observations $V = \{v_1, v_2, \dots, v_M\}$, representing the observations corresponding to the system's actual output.

Additionally, the system is governed by two probability measures π and $a_{i,j}$. The probability measure $\pi = \{\pi_i\}$ signifies the probability of $q_1 = S_i$ at initialization. The probability measure $a_{i,j}$ defines the probability of transition between any pair of states i and j . The transition probability from state i to state j is summarized in a transition matrix \mathbf{A} as seen in (1).

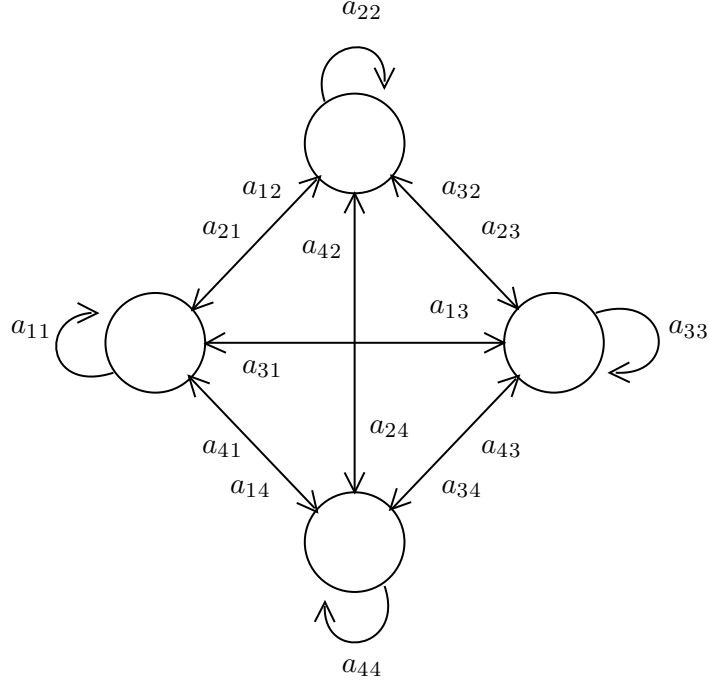


Figure 4: Four state HMM model with transitions between all states i.e., $a_{ij} \geq 0$

$$A = \{a_{i,j}\} = \begin{bmatrix} a_{1,1} & a_{1,2} & a_{1,3} & a_{1,4} \\ a_{2,1} & a_{2,2} & a_{2,3} & a_{2,4} \\ a_{3,1} & a_{3,2} & a_{3,3} & a_{3,4} \\ a_{4,1} & a_{4,2} & a_{4,3} & a_{4,4} \end{bmatrix} \quad (1)$$

Note that the transition probabilities comply with standard stochastic constraints and therefore have the following characteristics: $\sum_{j=1}^N a_{ij} = 1$, and it is typically assumed that transitions between any pair of states i and j are possible; hence $a_{ij} > 0$.

The last probability measure is the emission probability within the state i , denoted as $B = \{b_j(k)\}$ (2), indicating the likelihood of observing v_k given that the system is in the state S_i at time t .

$$b_j(k) = \mathbf{P}[v_k \text{ at } t | q_t = S_i], \quad 1 \leq j \leq N, \quad 1 \leq k \leq M \quad (2)$$

Given these elements of the HMM, two model hyper-parameters, N and M , along

with the specification of observation symbols, and the definition of the measures A , B , and π , are required in order to estimate the model. For convenience, a compact notation $\theta = (A, B, \pi)$ (3) can be used to denote the complete set of parameters of the model.

$$\theta = (A, B, \pi) \quad (3)$$

3.2.1 Forward-Backward Procedure

The preceding section on HMM raises the challenge of efficiently computing $\mathbf{P}(\mathbf{O}|\theta)$ given an observation sequence $\mathbf{O} = \mathbf{O}_1, \mathbf{O}_2, \dots, \mathbf{O}_T$, where each \mathbf{O}_i corresponds to a set of observations v . For this paper, \mathbf{O}_i is the observed CPI and GDP growth at a given period of time. The process of computing $\mathbf{P}(\mathbf{O}|\theta)$ is essential when we estimate the parameters of the model by fitting it to the data using the Baum-Welsh algorithm.

The process is initiated by defining the forward variable $\alpha_t(i)$ (4), which denotes the probability of the partial observation sequence $\mathbf{O}_1\mathbf{O}_2\dots\mathbf{O}_t$ up to time t and being in state S_i at time t , given the model parameters θ .

$$\alpha_t(i) = \mathbf{P}(\mathbf{O}_1, \mathbf{O}_2, \dots, \mathbf{O}_t, q_t = S_i | \theta) \quad (4)$$

Initially, the forward procedure is bootstrapped with (5), which defines the joint probability of being in state S_i and observing \mathbf{O}_1 . Subsequently, (6) is employed to determine how state S_j at time $t + 1$ can be reached from N possible states S_i , where $1 \leq i \leq N$. Given that $\alpha_t(i)$ represents the joint probability of observing $\mathbf{O}_1, \mathbf{O}_2, \dots, \mathbf{O}_t$ while in state S_i at time t , and transitioning to state S_j at time $t + 1$ from state S_i at time t , it can be expressed simply as $\alpha_t(i)a_{ij}$, which then enables determination of $\mathbf{P}(\mathbf{O}|\theta)$ (7).

$$\alpha_1(i) = \pi_i b_i(\mathbf{O}_1), \quad 1 \leq i \leq N \quad (5)$$

$$\alpha_{t+1}(j) = \left[\sum_{i=1}^N \alpha_t(i) a_{ij} \right] b_j(\mathbf{O}_{t+1}), \quad \begin{array}{l} 1 \leq t \leq T - 1 \\ 1 \leq j \leq N \end{array} \quad (6)$$

$$\mathbf{P}(\mathbf{O}|\lambda) = \sum_{i=1}^N \alpha_T(i) \quad (7)$$

The backward procedure is initiated by defining the backward variable $\beta_t(i)$, which denotes the probability of the observation sequence $\mathbf{O}_{t+1}, \mathbf{O}_{t+2}, \dots, \mathbf{O}_T$ given the current state S_i and model parameters θ (8).

$$\beta_t(i) = \mathbf{P}(\mathbf{O}_{t+1}, \mathbf{O}_{t+2}, \dots, \mathbf{O}_T | q_t = S_i, \theta) \quad (8)$$

Subsequently, the backward procedure is initialized with (9). Then, an induction function is defined (10) that shows that having been in state S_i at time t , and to account for the observation sequence from $t + 1$, all possible states S_j at time $t + 1$ are considered, taking into account the transition from S_i to S_j , as well as the observation \mathbf{O}_{t+1} in state j , and subsequently accounting for the remaining partial observation sequence from state j .

$$\beta_T(i) = 1, \quad 1 \leq i \leq N \quad (9)$$

$$\beta_t(i) = \sum_{j=1}^N a_{i,j} b_j(\mathbf{O}_{t+1}) \beta_{t+1}(j), \quad t = T - 1, T - 2, \dots, 1, \quad 1 \leq i \leq N \quad (10)$$

3.2.2 Viterbi Algorithm

The Forward-Backward procedure does not address how to compute the "optimal" state sequence given a specific observation sequence, which presents an additional challenge of defining an optimality criterion. Utilizing the Viterbi algorithm (Viterbi, 1967; Forney, 1973) it is possible to identify the most likely state sequence, equivalent to maximizing $\mathbf{P}(Q, \mathbf{O} | \theta)$.

To find the most likely state sequence $Q = \{q_1 q_2 \dots q_T\}$ given the observation sequence $\mathbf{O} = \{\mathbf{O}_1 \mathbf{O}_2 \dots \mathbf{O}_T\}$, we need to define (11), that is, the highest probability along a path at time t , which accounts for the t first observations and ends in state S_i .

$$\delta_t(i) = \max_{q_1, q_2, \dots, q_{t-1}} \mathbf{P}[q_1 q_2 \dots q_t = i, \mathbf{O}_1 \mathbf{O}_2 \dots \mathbf{O}_t | \theta] \quad (11)$$

Hence, the induction process becomes (12). Where $a_{i,j}$ represents the transition probability from state $i \rightarrow j$ and $b_j \mathbf{O}_{t+1}$ is the emission probability for \mathbf{O}_{t+1} .

$$\delta_{t+1}(j) = [\max_i \delta_t(i) a_{i,j}] * b_j(\mathbf{O}_{t+1}) \quad (12)$$

In order to retrieve the state sequence, it is necessary to track the argument which maximizes (12), for each t and j . The argument that maximizes the induction function for each t and j is stored in the array $\psi_t(j)$ (13b). The remainder of the procedure to find the optimal state sequence is specified in (13a) - (16). The procedure follows a similar process to that of the forward procedure as shown in section 3.2.1.

$$\delta_1(i) = \pi_i b_i(\mathbf{O}_1), \quad 1 \leq i \leq N \quad (13a)$$

$$\psi_1(i) = 0 \quad (13b)$$

$$\delta_t(j) = \max_{1 \leq i \leq N} [\delta_{t-1}(i) a_{ij}] b_j(\mathbf{O}_t), \quad \begin{array}{l} 2 \leq t \leq T \\ 1 \leq j \leq N \end{array} \quad (14a)$$

$$\psi_t(j) = \arg \max_{1 \leq i \leq N} [\delta_{t-1}(i) a_{ij}], \quad \begin{array}{l} 2 \leq t \leq T \\ 1 \leq j \leq N \end{array} \quad (14b)$$

$$\mathbf{P}^* = \max_{1 \leq i \leq N} [\delta_T(i)] \quad (15a)$$

$$q_T^* = \arg \max_{1 \leq i \leq N} [\delta_T(i)] \quad (15b)$$

$$q_t^* = \psi_{t+1}(q_{t+1}^*), \quad t = T-1, T-2, \dots, 1 \quad (16)$$

The primary distinction from the forward procedure lies in the maximization in (14a), which is used instead of the summation procedure in the forward procedure.

3.2.3 Baum-Welch Algorithm

When estimating the parameters by fitting the model to the data, we rely on an iterative procedure known as the Baum-Welch algorithm. This algorithm returns a local maximum for $\mathbf{P}(\mathbf{O}|\theta)$ by adjusting the model parameters (A, B, π) accordingly. Firstly, we define $\xi_t(i, j)$ (17), which denotes the probability of being in state S_i at time t and state S_j at time $t+1$ given the observed sequence and the model specification.

$$\xi_t(i, j) = \mathbf{P}(q_t = S_i, q_{t+1} = S_j | \mathbf{O}, \theta) \quad (17)$$

Using the definitions of the forward and backward variables (4) (8), we can write $\xi_t(i, j)$ as (18):

$$\xi_t(i, j) = \frac{\alpha_t(i) a_{ij} b_j(\mathbf{O}_{t+1}) \beta_{t+1}(j)}{\mathbf{P}(\mathbf{O} | \theta)} = \frac{\alpha_t(i) a_{ij} b_j(\mathbf{O}_{t+1}) \beta_{t+1}(j)}{\sum_{i=1}^N \sum_{j=1}^N \alpha_t(i) a_{ij} b_j(\mathbf{O}_{t+1}) \beta_{t+1}(j)} \quad (18)$$

Furthermore, $\gamma_t(i)$ is defined as the probability of being in state S_i at time t given the model specification and the observation sequence. By summing over j , $\gamma_t(i)$ can be related to $\xi_t(i, j)$.

$$\gamma_t(i) = \frac{\alpha_t(i) \beta_t(i)}{\sum_{i=1}^N \alpha_t(i) \beta_t(i)} \rightarrow \gamma_t(i) = \sum_{j=1}^N \xi_t(i, j) \quad (19)$$

If $\gamma_t(i)$ is summed over time excluding the last period T , i.e., $\sum_{t=1}^{T-1} \gamma_t(i)$ a quantity is obtained that can be interpreted as the expected amount of times that state S_i is visited, or equivalently the expected number of transitions from state S_i . Similarly, via summing $\xi(i, j)$ over time (excluding the last period T), that is, $\sum_{t=1}^{T-1} \xi_t(i, j)$ can be interpreted as the number of transitions from state S_i to state S_j . Using this principle of counting occurrences as well as the formulas mentioned above, it becomes possible to estimate the HMM parameters using the functions seen in (20) - (22) (Rabiner, 1989).

$$\hat{\pi}_i = \gamma_1(i) \quad (20)$$

$$\hat{a}_{ij} = \frac{\sum_{t=1}^{T-1} \xi_t(i, j)}{\sum_{t=1}^{T-1} \gamma_t(i)} \quad (21)$$

$$\hat{b}_j(k) = \frac{\sum_{t=1}^T \xi_t(i, j)}{\sum_{t=1}^T \gamma_t(j)} \quad (22)$$

Using the initial model parameters $\theta = (A, B, \pi)$ to compute the right-hand side of Equations (20) - (22), and subsequently defining the re-estimated model $\hat{\theta} = (\hat{A}, \hat{B}, \hat{\pi})$ using the left-hand side of Equations (20) - (22), Baum (1968) and Baker (1975) have shown that either the initial model (θ) defines a critical point, implying $\theta = \hat{\theta}$, or the model $\hat{\theta}$ returns a higher probability, i.e. $\mathbf{P}(\mathbf{O} | \hat{\theta}) > \mathbf{P}(\mathbf{O} | \theta)$ meaning that the new estimated

parameters is a more likely fit to the data. Thus, through an iterative procedure, the local maxima for the maximum likelihood of the HMM can be determined.

3.2.4 Gaussian HMM

The estimation process of an HMM described above assumes that the observations are from a finite set, for example, the alphabet in language models. In order to incorporate the estimation procedure to accommodate continuous observations, namely, those not comprised of discrete observations from a finite set, it becomes necessary to impose certain constraints upon the model's probability density function (PDF). Liporace (1982), Juang (1985) and Juang et al. (1986) provides a method for re-specifying the PDF (23) which accommodates consistent estimation of the model parameters while having continuous observations.

$$b_j(\mathbf{O}) = \sum_{m=1}^M c_{jm} \mathfrak{R}[\mathbf{O}, \mu_{jm}, \mathbf{U}_{jm}], \quad 1 \leq j \leq N \quad (23)$$

Here, \mathbf{O} denotes the observations under consideration, c_{jm} represents the m -th mixture in state j , and \mathfrak{R} denotes any log-concave or elliptically symmetric density (Liporace, 1982), characterized by a mean vector μ_{jm} and a covariance matrix \mathbf{U}_{jm} . Crucially, it is noted that the mixture component c_{jm} conforms to the stochastic constraints presented in (24a)–(24b).

$$\sum_{m=1}^M c_{jm} = 1, \quad 1 \leq j \leq N \quad (24a)$$

$$c_{jm} \geq 0, \quad 1 \leq j \leq N, \quad 1 \leq m \leq M \quad (24b)$$

This ensures the proper normalization of the PDF, as presented in (25).

$$\int_{-\infty}^{\infty} b_j(x) dx = 1, \quad 1 \leq j \leq N \quad (25)$$

Liporace (1982), Juang (1985), and Juang et al. (1986), show how the estimation of the coefficients in the mixture density (c_{jm} , μ_{jm} , \mathbf{U}_{jm}) specifies to the formulations presented in (26)–(28).

$$\hat{c}_{jk} = \frac{\sum_{t=1}^T \gamma_t(j, k)}{\sum_{t=1}^T \sum_{k=1}^M \gamma_t(j, k)} \quad (26)$$

$$\hat{\mu}_{jk} = \frac{\sum_{t=1}^T \gamma_t(j, k) \mathbf{O}_t}{\sum_{t=1}^T \gamma_t(j, k)} \quad (27)$$

$$\hat{\mathbf{U}}_{jk} = \frac{\sum_{t=1}^T \gamma_t(j, k) (\mathbf{O}_t - \mu_{jk})(\mathbf{O}_t - \mu_{jk})^T}{\sum_{t=1}^T \gamma_t(j, k)} \quad (28)$$

Here, $\gamma_t(j, k)$ denotes the probability of being in state j at time t , with the k -th mixture component accounting for the observation sequence \mathbf{O} (29).

$$\gamma_t(j, k) = \left[\frac{\alpha_t(j) \beta_t(j)}{\sum_{j=1}^N \alpha_t(j) \beta_t(j)} \right] \left[\frac{c_{jk} \mathfrak{R}(\mathbf{O}_t, \mu_{jk}, \mathbf{U}_{jk})}{\sum_{m=1}^M c_{jm} \mathfrak{R}(\mathbf{O}_t, \mu_{jm}, \mathbf{U}_{jm})} \right] \quad (29)$$

The meaning of (26)–(28) is relatively clear (Rabiner, 1989). Estimating the mixture component c_{jk} involves calculating the ratio between the expected number of times the system occupies the state j using the k -th mixture component and the expected number of times the system is in state j . Similarly, the mean vector μ_{jk} weighs each term in the numerator of (26) using the observation vector \mathbf{O} , providing the expected value of the segment of the observation vector corresponding to the component of the k -th mixture. Likewise, the re-estimation of the covariance matrix is interpreted similarly to the mean vector.

3.3 Fitting of Hidden Markov Models

The fitting procedure for Hidden Markov Models (HMMs) begins with specifying the desired HMM structure, including the number of hidden states and the emission distribution (Robles et al., 2012). After initializing the model, the Baum-Welch algorithm is used to iteratively adjust the transition and emission probabilities, maximizing the likelihood of observed data given the model (Nguyen, 2018). In this paper the fitting process is executed using the fit method provided by the HMMlearn python library.

Once the model is fitted, the log-likelihood of the observed data under the model can be computed, providing a measure of how well the model explains the data. However, relying solely on the log likelihood can lead to over-fitting, as it often increases with the number of parameters. This is where the Akaike Information Criterion (AIC) (30) proves

invaluable.

$$AIC = 2k - 2\ln(\hat{L}) \quad (30)$$

The AIC accounts not only for the model's goodness of fit, i.e., log-likelihood (\hat{L}) but also introduces a penalty based on the number of parameters in the model (k). By penalizing models with more parameters, the AIC promotes a balance between model complexity and fit, helping to identify models that generalize better to new data. Thus, models with more parameters that might simply overfit the training data are penalized, leading to the selection of models that best capture the underlying structure without excessive complexity (Akaike, 1974). Psaradakis and Spagnolo (2003) highlight this principle when determining the optimal number of regimes in Markov-switching models, emphasizing that using criteria like AIC effectively balances model accuracy and complexity, ensuring that the chosen model adequately captures the regime-switching behavior in time-series data without over-fitting.

3.3.1 Model Evaluation

To evaluate the performance of the Hidden Markov Model, Monte Carlo simulations with two settings are implemented. Through a data generation procedure defined in Section 4.1 a sample is generated. We also evaluate the HMM against a random walk in both the simulated setting and when fitting the model to real data. The Monte Carlo approach allows for assessment regarding the robustness of the model's transition and emission probabilities, providing a measure of how well the model generalizes across different state sequences. By comparing the likelihood scores of the observed data between the different settings, the analysis can reveal potential over-fitting or under-fitting issues, ensuring that the model truly captures the underlying dynamics of the data rather than simply conforming to specific patterns in the training data set. The usage of a random walk as a benchmark also enables evaluation of statistical measurements which in isolation are uninformative and hence difficult to evaluate.

3.4 Portfolio Construction

We construct eight different portfolios (see Table 1), using seven different ETFs. Two of the eight portfolios, namely the Simple EW and RP portfolios, serve primarily as a benchmark. In addition to these benchmark portfolios, an additional two static portfolios are created using either the risk-parity or equal weighted methods for allocation. The layered EW and RP portfolios are created to have an equal exposure towards each market regime in terms of either risk or ratio of the portfolio. The remaining four portfolios are constructed to dynamically adjust their exposure towards any market regime in accordance to the relative likelihood as predicted by the HMM.

Table 1: Summary of each portfolio and the weighting method used.

Portfolio Notation	Subportfolio Weighting	Main Portfolio Weighting	Layers	Portfolio Type
Simple EW	NA	Equal Weights	1	Static
Simple RP	NA	Risk Parity	1	Static
Layered EW	Equal Weights	Equal Weights	2	Static
Layered RP	Risk Parity	Risk Parity	2	Static
HMM EW	Equal Weights	HMM	2	Dynamic
HMM RP	Risk Parity	HMM	2	Dynamic
HMM EW EMA	Equal Weights	smoothed HMM	2	Dynamic
HMM RP EMA	Risk Parity	smoothed HMM	2	Dynamic

In all portfolios consisting of two layers, four distinct state optimal portfolios, or sub-portfolios, are constructed using the equally weighted or risk-parity methodologies (see Figure 5). The dual layered static portfolios keep a constant exposure towards each market in terms of risk or ratio of portfolio by re-balancing the allocation of each sub-portfolio in the overarching main portfolio on a monthly basis. The allocation towards each sub-portfolio in the static main portfolio is determined by either the equal weighted or risk-parity methodology. The dynamic portfolios differ in their usage of estimated probabilities from the HMM to adjust the exposure towards each sub-portfolio. The dynamic portfolios are also re-balanced on a monthly basis according to the updated HMM estimates. Each portfolio construction is explained in depth below.

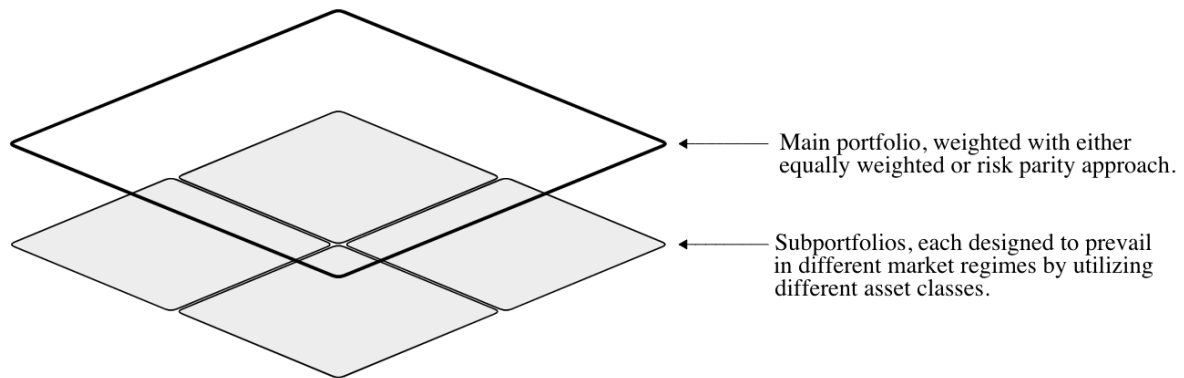


Figure 5: Dual layered portfolios construction with a sub-portfolio layer, where each sub-portfolio is optimized for respective market regime, followed by a main portfolio utilizing either the equally weighted or risk parity approach for the four sub-portfolios.

3.4.1 Equally Weighted Portfolio Construction

As an initial benchmark portfolio, a simple monthly re-balanced equally weighted diversification strategy is implemented. Initially, each asset corresponds to a total of $1/N$ of the portfolio, where N denotes the number of assets in the portfolio. The implementation is consistent with Plyakha et al. (2012) and effectively provides a simple exposure to each asset.

3.4.2 Risk Parity Portfolio Construction

This section describes the computational approach used to build a risk-parity benchmark portfolio, which aims to equalize the risk contributions of each asset in the portfolio. The methodology is grounded on the framework outlined by Fisher et al. (2015); Qian (2011).

The variance of the portfolio is computed using (31). Portfolio variance is computed under the assumption of normally distributed returns, but any distribution \mathcal{D} with finite covariance is sufficient. The assumption of normality is preferred due to simplicity and implications when computing Sharpe ratios.

$$\sigma_{Portfolio}^2 = \omega^T \Sigma \omega \quad (31)$$

where ω represents the vector of asset weights and Σ is the covariance matrix, calculated on daily asset returns over the previous twelve months.

In order to determine how each asset contributes risk to the portfolio, we compute the marginal risk contribution (MRC) of each asset (32).

$$MRC = \frac{\Sigma\omega}{\sigma_{Portfolio}^2} \quad (32)$$

Following this, individual risk contributions (RC) from each asset can be determined by (33).

$$RC = \omega \cdot MRC \quad (33)$$

The objective function of optimization is to minimize the sum of squared deviations of individual risk contributions from their mean (target risk), which promotes risk parity across the portfolio (34). We subject the optimization to a normalization constraint, that is, $\sum_{i=1}^N \omega_i = 1$ and forbid short selling, $0 \leq \omega_i \leq 1$.

$$Objective = \sum (RC - \overline{RC})^2 \quad (34)$$

This objective aligns with the risk-parity approach by ensuring that all assets contribute equally to the total risk of the portfolio.

3.4.3 Dual Layered Static Portfolios

In the static portfolios consisting of two layers, four different state-optimal sub-portfolios are constructed using the equal or risk-parity weighting method (see Figure 5). Each sub-portfolio is designed to perform well in a specific market regime by including assets that have been shown to perform well in the given regime. Due to the limitations of this study, the construction of each sub-portfolio, with regard to the optimal asset classes in each market regime, is based on previous findings and recommendations of Shahidi and Lee (2014) and Bridgewater (2009).

Within the equally weighted layered portfolios, we individually create the sub-portfolios by setting the weight of each ETF to $1/N$. The four sub-portfolios are then combined into a main portfolio, where each sub-portfolio constitutes 25%.

The layered risk-parity portfolio similar to the layered equally weighted portfolio requires the construction of four sub-portfolios. Using the same asset within each sub-portfolio as in the equally weighted layered portfolio, we calculate new weights using the risk-parity method. The four risk-parity sub-portfolios are subsequently combined to

create the overarching main portfolio. The weight of each sub-portfolio within the main portfolio is determined using the risk-parity method.

Both static layered portfolios are re-balanced on a monthly basis in both the sub- and main portfolio layers. This ensures a static exposure in terms of risk or ratio towards each market regime over time.

3.4.4 Hidden Markov Model for Dynamic Weighting

The dynamic portfolios also require the use of sub-portfolios. These are built using either the risk-parity or equal-weighted methods in the same manner as the static layered portfolios. Subsequently, the sub-portfolios are dynamically adjusted within the main portfolio according to the relative estimated probability $\hat{\gamma}_t(j, k)$ for a given regime j at time t . The regime probabilities are estimated on CPI and GDP data and are updated on a monthly basis, and the exposure towards each market regime is hence adjusted. Similarly, each sub-portfolio is re-balanced on a monthly frequency.

$$\omega_{j,t} = \hat{\gamma}_t(j, k) \quad (35)$$

3.4.5 Smoothed Dynamic Weights

Inherent to the HMM portfolios are fluctuations in the weights due to sudden shifts in probabilities. To ease these rapid fluctuations an exponentially weighted moving average (EWMA) approach is implemented, utilizing a smoothing parameter $\alpha = \frac{2}{\text{span}+1}$. This approach limits the impact of new data, and thus the weights become more stable over time. For simplicity a span of three periods is utilized, resulting in $\alpha = 0.5$. Smoothed weights are defined by (36), where ω_t^* denotes the smoothed weights.

$$\omega_t^* = \alpha * \omega_t + (1 - \alpha) * \omega_{t-1}^* \quad (36)$$

After smoothing, the weights are normalized (37) to ensure they sum to unity.

$$\omega_t^* = \frac{\omega_{t,i}^*}{\sum_{i=1}^N \omega_{t,i}^*} \quad (37)$$

3.5 Performance Measures

Each portfolio is assessed through various performance metrics chosen to reflect different dimensions of the performance. The metrics used in evaluation are the following: Sharpe Ratio, multi-factor alphas and drawdowns. We also adjust the return for each portfolio to account for transaction cost occurring when re-balancing.

The Sharpe ratio (SR) (38), measuring the relation between risk and return is used to give an intuitive sense of the return relative to the risk exposure of each portfolio.

$$SR = \frac{E(r) - r_f}{\sigma_p}. \quad (38)$$

To provide further evidence and to ensure that the study is comparable with current research, a factor model is applied to calculate multi-factor alphas as a risk adjusted performance measure (39). Following Bessler et al. (2021), the factor model embraces the six Fama-French factors (Novak et al., 2022), available on Kenneth French's website. The factors used are the following. Market Excess Return ($R_m - r_f$), Small Minus Big (SMB), High Minus Low (HML), Robust Minus Weak (RMW), Conservative Minus Aggressive (CMA) and Momentum (WML). Through this analysis, all portfolios are evaluated to determine whether the returns can be explained with these established risk factors or whether the model portfolios actually provide substantial alphas. It is worth mentioning that other factor models, which are more frequently used in the assessment of multi-asset portfolios, could have been employed. However, given the constraints we subject the portfolio to is typically observed in mutual funds, it is suitable to assess the portfolios using the conventional factor model for such funds.

$$r_{i,j} = \alpha + \beta_1(R_m - r_f)_t + \beta_2SMB_t + \beta_3HML_t + \beta_4RMW_t + \beta_5CML_t + \beta_6WML_t + \epsilon_t \quad (39)$$

The "drawdown" defined as the accumulated percentage loss resulting from a sequence of drops in the price of an investment is calculated according to (40).

$$\text{Drawdown}_t = \frac{P_t - \max_{\tau \leq t} P_\tau}{\max_{\tau \leq t} P_\tau} \quad (40)$$

where:

- P_t is the portfolio value at time t .
- $\max_{\tau \leq t} P_\tau$ is the highest value achieved by the portfolio up to time t .

This formula calculates the drawdown as a percentage of the maximum value of the portfolio, providing a measure of the relative decline from the highest point reached by the portfolio. The maximum drawdown (MDD) (41) that occurs on a fixed investment horizon, i.e., the entire out-of-sample period, provides a different perception of the risk and price flow of an investment without any requirement regarding the distribution of returns (Grossman and Zhou, 1993), highlighting the peak-to-trough decline before the investment returns to its previous peak value (Leal and de Melo Mendes, 2005).

$$\text{MDD}_i = \text{Max}_{i,t^* \in (0,T)} \left[\text{Max}_{i,t \in (0,t^*)} \left(\frac{P_{i,t} - P_{i,t^*}}{P_{i,t}} \right) \right] \quad (41)$$

Since all portfolios are re-balanced with a monthly frequency, the real-world implementation of our portfolios would accumulate transaction costs. We account for this by penalizing the return of each portfolio in proportion to the size of each re-balancing (42). In accordance with the transaction cost on Avanza and Nordnet we set the transaction cost to 89 basis points ($v = 0.0089$).

$$TC_{i,t} = \sum_{j=1}^N (|\omega_{i,j,t+1} - \omega_{i,j,t}|)v, \quad (42)$$

4 Monte Carlo

To evaluate the statistical robustness and viability in modeling the macroeconomic environment, two different Monte Carlo simulations are implemented. The first simulation generates a new state sequence for each iteration while the second simulation utilizes the same state sequence for each iteration.

4.1 Sample Generation

The method involves defining a domain of possible inputs, which are randomly generated from a probability distribution. The generation of a state sequence can be done using the HMM (Roman et al., 2010). The generation of random state sequences is initialized by selecting an initial state from the probability distribution π . For this simulation study, the initial state probability is set to $\pi = [0.25 \ 0.25 \ 0.25 \ 0.25]$. Then, using the transition matrix \mathbf{A} specified in (43), the subsequent states in the series are randomly generated.

$$A = \{a_{i,j}\} = \begin{bmatrix} 0.9 & 0.04 & 0.04 & 0.02 \\ 0.04 & 0.9 & 0.04 & 0.02 \\ 0.02 & 0.04 & 0.9 & 0.04 \\ 0.02 & 0.04 & 0.04 & 0.9 \end{bmatrix} \quad (43)$$

From each state, we generate continuous observations for CPI and GDP using the mean vector μ and the covariance vector Σ . The vector μ defines the means of the two variables in four different states, consistent with the visual representation in Figure 1. The emission probability, i.e. the probability of observing X while in state S_j at time t is used to generate a sequence of observable values. For the emission probability, the mean and covariance vectors constitute the basis from which a standard maximum likelihood estimator for a Gaussian distribution (44) is utilized to draw a sequence of observable values.

$$\mathbf{P}[X|S_j = q_t] = \frac{1}{\sqrt{(2\pi)^k |\Sigma_j|}} \exp\left(-\frac{1}{2}(X - \mu_j)^T \Sigma_j^{-1} (X - \mu_j)\right) \quad (44)$$

We define a mean vector μ , using the 25th and 75th percentile in the CPI and GDP data to obtain two levels of the means, specifically $\mu_{CPI} = [1.8 \quad 3.7]$ and $\mu_{GDP} = [3.8 \quad 6.1]$. These can then be sorted into four different states. The covariance matrix is defined to mimic a standard normal distribution, $\Sigma = 0.5 * \mathbf{I}_{2,2}$, where \mathbf{I} is a two-dimensional identity matrix. This produces observations with the same variance and no correlation across dimensions between the CPI and GDP. This means that each observable variable will be drawn from a Gaussian distribution, $\mathcal{N} \sim (\mu_j, \Sigma_j)$. Although variables are independent across dimensions, they are temporally correlated through the transition matrix \mathbf{A} . The transition matrix does not affect the covariance matrix between different states directly but rather imposes a correlation by affecting the likelihood of being in a specific state at a given time, based on the previous state. Given how the state sequence indirectly affects the observations, it is thus ensuring a temporal correlation.

This approach is sufficient in producing a sample that is a good approximation of the macroeconomic environment in stable times, but struggles with anomalies, such as market crashes (Messina and Toscani, 2008). Although consideration must be given to the limitations of the approach, the fact that Monte Carlo simulation produces an estimate of the distribution of outcomes is a valuable input in determining the viability of the suggested model (Glasserman and Merener, 2003).

Using the sample generation procedure, two different settings are used in the simulations. The first setting generates a new state sequence for each iteration, which then constitutes the base for generating the observable variables for CPI and GDP, called Monte Carlo 1. In the second setting, each simulation uses the same state sequence but generates a new sequence of observable values for CPI and GDP for each iteration, called Monte Carlo 2. The second setting allows us to plot the probability estimates along with the distribution of estimates over all iterations.

4.2 Monte Carlo Results

Table 2 presents the results of both settings in the simulation, as well as the data evaluated on a random walk, where each measurement provides valuable insight into a

different components of the models performance in the two different settings. The average Root Mean Squared Error (RMSE) measures the average error in the estimated state probabilities and true states, where a lower RMSE indicates a closer fit to the data. The RMSE for the estimated CPI and GDP, determined by the means in the most probable state compared to the observed data, is also computed. The average Akaike Information Criterion (AIC), on the other hand, evaluates the trade-off between goodness of fit and model complexity. A lower AIC suggests that the model more efficiently explains the variability in the data by using less parameters. The Log Likelihood provides a measure of model accuracy by computing the likelihood of the observed data given the model.

Table 2: Summary of the two different Monte Carlo settings and teh random walk performance in a simulated environment. Monte Carlo 1 & 2 indicates the first and second setting respectively.

	RMSE	RMSE CPI	RMSE GDP	AIC	Log Likelihood	Accuracy
Random Walk	-	0.0169	0.0191	-	-	-
Monte Carlo 1	0.1021	0.0070	0.0072	1102.6466	-516.4154	0.9672
Monte Carlo 2	0.0789	0.0060	0.0074	1086.2207	-508.1104	0.9823

By comparing the outcomes from the two simulation settings to the random walk, it becomes apparent that within the simulated environment the HMM effectively maps the output of the hidden states. For the CPI and GDP estimation, the HMMs produce more favorable RMSE values, indicating the model’s ability to accurately measure the CPI and GDP levels.

In the second simulation, stability in the estimated probabilities for a given state during periods without regime shifts is observed (see Figure 6). The stability in approximately the first three quarters of the sequence suggests a consistent and predictable pattern in the underlying data, which the HMM accurately captures. However, as a regime shift is approached, an increased spread in the estimated probabilities across the iterations is identified. The increased spread suggests an elevated uncertainty and difficulty in accurately predicting the current state. This is an expected effect, as the increased uncertainty implies that the model captures a shift in the underlying data and starts to adjust its predictions accordingly. For most regime shifts, the model is timely in adjusting its estimated probabilities, however, for short temporary regime shifts the adjustments are less precise.

The increased uncertainty in the last quarter of the sequence implies an unfavorable tendency when regimes are short and switch frequently. This finding has negative implications for portfolio construction. Because of the unpredictable forecasts, using HMM probabilities in portfolio allocation could negatively affect the portfolio by tilting it towards assets that are negatively influenced by the prevailing market conditions. Therefore, during times of rapid and frequent regime changes, this Monte Carlo simulation indicates that the use of HMM state probabilities is sub-optimal.

Despite the fact that the model faces challenges in forecasting short-term and brief regimes, its overall timely and accurate predictions within the simulated environment indicate that it can identify hidden states and potentially provide upside in creating a dynamic investment strategy.

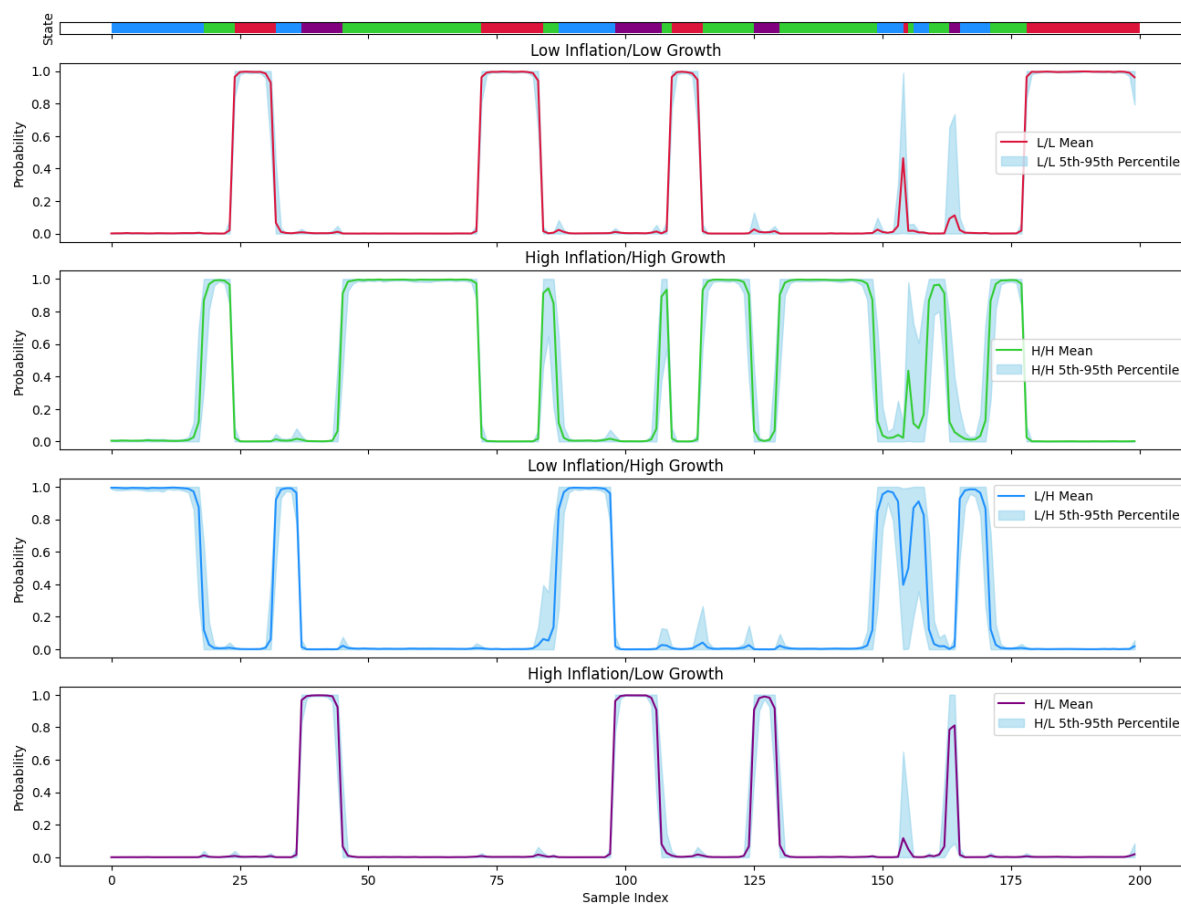


Figure 6: Probabilities for the four different market regimes over time in a simulated environment. The shaded area represents the 5th and 95th percentile in estimated probability.

5 Data

We use five different asset classes, which can be invested in through seven ETFs. The ETFs are presented in Table 3. Daily price data for the seven ETFs are downloaded from S&P Capital IQ and Stooq for the period January 1, 2014 - January 2, 2024. This results in a data set of 2516 daily return observations for each ETF. The monthly CPI and GDP data is retrieved from S&P Global for the period January 1, 1992 - December 31, 2023. The year-on-year (YoY) GDP growth is computed, which cuts the sample by one year. This results in a sample of macroeconomic variables spanning the period January 1, 1993 - December 31, 2023.

Table 3: Description of ETFs and asset classes

Ticker	ETF Name	Asest Class
DBC	Invesco DB Commodity Index Tracking Fund	Commodities
GLD	SPDR Gold Shares	Gold
IEI	iShares 3-7 Year Treasury Bond	Treasury Bonds
TIP	iShares TIPS Bond	Treasury Inflation Protected Securities
TLT	iShares 20+ Year Treasury Bond	Treasury Bonds
VCIT	Vanguard Intermediate-Term Corp Bond	Corporate Bonds
VOO	Vanguard S&P 500	Equity

Looking at the YoY change in CPI and GDP (Figure 7), we observe a relatively stable macroeconomic environment up to approximately 2008. Nevertheless, during the 2007 financial crisis, a decline in both CPI and GDP growth is observed. The macroeconomic environment then stabilizes again up until the outbreak of the pandemic in 2020. Coinciding with Covid-19 in 2020 the GDP initially drops rapidly to then recover and shoot up. The CPI on the other hand remains stable until 2021 and then begin to rise steadily. Towards the end of the time-series both the CPI and GDP have begun to revert back to levels similar to the beginning of the series.

Looking at the cumulative return and the CAGR for each asset during the time period (see Figure 8 and Table 4), we observe that only the 'VOO' and 'GLD' ETFs produce a positive return. The remaining ETFs are relative stable during the time period except for 'DBC' which initially dips to then recover.

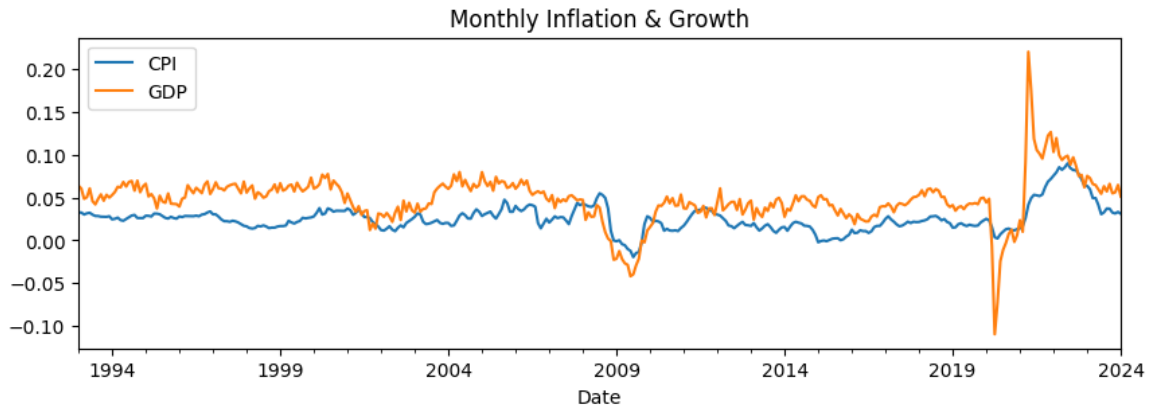


Figure 7: CPI and GDP over time.

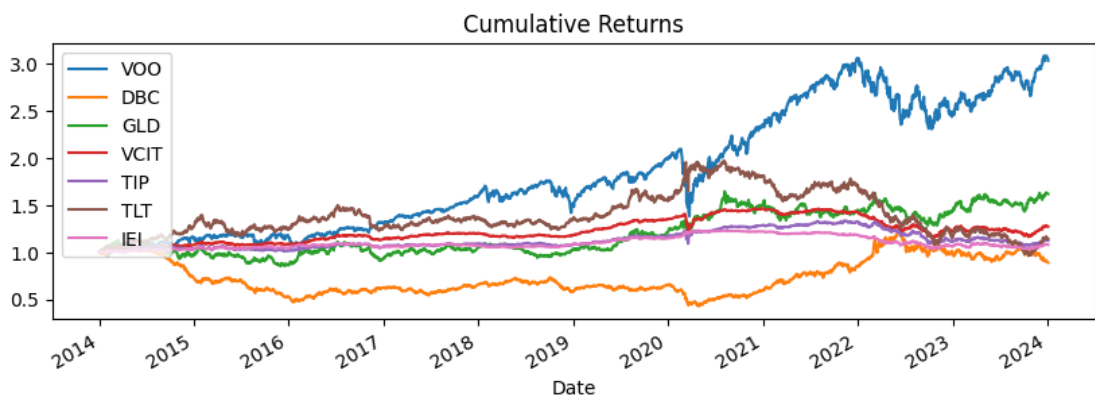


Figure 8: Cumulative return for each ETF

Table 4 presents the statistical properties of the daily returns generated by each ETF. Average daily return ranges from -0.01% ('IEI') to 0.04% ('VOO'). The equity ETF ('VOO') have both the minimum and maximum value, -11.74% and 9.54% . Comparison of the standard deviation among the ETFs reveals that 'IEI' has the lowest risk, in terms of standard deviation at 0.24% , and 'DBC' the highest at 1.12% .

The correlation structure among the assets is one of the most essential statistical properties that directly affects risk, and thus the performance of the portfolio. Since a correlation structure with weakly correlated assets offers superior diversification possibilities. Importantly, a more diversified portfolio does not necessarily imply higher returns. From Panel B in Table 4 we can determine the highest correlation pairs as the following: 'IEI' - 'TLT' (0.80), 'IEI' - 'VCIT' (0.74) and 'IEI' - 'TIP' (0.73). The pairs with the lowest negative correlation are the following: 'TLT' - 'VOO' (-0.24), 'IEI' - 'VOO' (-0.17) and 'TLT' - 'DBC' (-0.17).

There are only two ETFs with positive CAGR ('VOO' & 'GLD'). Hence, they are

also the only two ETFs which produce positive Sharpe ratios. Expanding the analysis of the ETFs by performing a factor analysis we find that 'GLD' is the only one that produces a positive alpha when regressed on the six Fama French factors (see A for the full regression).

With respect to the portfolio construction process, the analysis of descriptive statistics produces a couple of takeaways. The on average relatively low correlation among assets should provide a solid foundation for creating a diversified portfolio. Furthermore, most average daily returns, along with the CAGR for each asset, are negative, potentially resulting in poor returns for portfolios that are restricted to these assets alone.

5.1 Sample Split

The sample is split into two sub-samples, training and test samples. The training sub-sample is used to fit and estimate the models, while the test sub-sample is used to evaluate the dynamic and strategies strategies out-of-sample performance. The training and test sub-samples for the CPI and GDP data are split into 78% and 22%, respectively. This split provides a sufficiently large data set in order to fit the model and still evaluate the performance out-of-sample. This results in the following time periods: January 1, 1993 - February 28, 2017 and March 1, 2017 - December 31, 2023

Table 4: Descriptive statistics for all ETFs. Mean, Std. Dev, Median, Min, Max, 25th & 75th percentile, Skewness and Kurtosis is calculated on daily returns for the full sample. CAGR is calculated using the cumulative return over the full sample. The Sharpe ratio is calculated using an annualized volatility and a risk free rate of 1.5%. Alpha is computed by regressing the daily returns against daily Fama-French six factors. The Correlation Matrix is based on daily returns for the full sample. (Significance Levels: * = 90%, ** = 95% & *** = 99%)

	DBC	GLD	IEI	TIP	TLT	VCIT	VOO
<i>Panel A: Summary Statistics</i>							
Mean	0,0008%	0,0231%	-0,0007%	-0,0003%	0,0032%	0,0000%	0,0443%
Std. Dev	1,1172%	0,8881%	0,2410%	0,3786%	0,9475%	0,3904%	1,1142%
Median	0,0639%	0,0343%	0,0000%	0,0091%	0,0412%	0,0119%	0,0589%
Min	-7,9444%	-5,3694%	-1,1183%	-2,8662%	-6,6683%	-4,4860%	-11,7388%
Max	4,7990%	4,9038%	1,4379%	4,4537%	7,5196%	5,4294%	9,5364%
25th Percentile	-0,5920%	-0,4652%	-0,1255%	-0,1866%	-0,5593%	-0,1693%	-0,3797%
75th Percentile	0,6217%	0,4895%	0,1264%	0,1949%	0,5525%	0,1858%	0,5675%
Skewness	-0,6142	-0,0084	-0,2857	0,1740	0,0918	0,3492	-0,5162
Kurtosis	4,0284	2,9225	3,5060	13,4243	4,8882	29,0081	15,0002
CAGR	-1,3666%	4,9452%	-0,2543%	-0,2542%	-0,3269%	-0,1936%	10,0551%
Sharpe Ratio	-0,1616	0,2444	-0,4586	-0,2919	-0,1215	-0,2733	0,4837
Alpha	-0,0049*** (0,000)	0,0048*** (0,000)	-0,0052*** (0,000)	-0,0052*** (0,000)	-0,0051*** (0,000)	-0,0052*** (0,000)	-0,0052*** (0,000)
Obs	2516	2516	2516	2516	2516	2516	2516
<i>Panel B: Correlation Matrix</i>							
DBC	1,0000						
GLD	0,2453	1,0000					
IEI	-0,0911	0,4123	1,0000				
TIP	0,1520	0,4002	0,7334	1,0000			
TLT	-0,1654	0,3121	0,8004	0,7133	1,0000		
VCIT	0,0739	0,3490	0,7374	0,6629	0,6576	1,0000	
VOO	0,3485	0,0181	-0,1665	0,0019	-0,2430	0,2016	1,0000

6 Empirical Results

This section presents the empirical results of the performance of our HMM in the out-of-sample period. We also report the out-of-sample results of the dynamic and static performance along with a robust analysis of the performance of all portfolios.

6.1 HMM results

HMM, when fitted to the data, provides the estimated transition matrix \hat{A} (45). What can be seen from the estimated probabilities along the diagonal is that regimes tend to have a high probability of continuing in the next time period. The low transition probabilities from state i to state j indicate that the regimes are sticky, and thus we can expect long periods of similar market environments. These insights are advantageous for a dynamic strategy, according to the results from Dahlquist and Harvey (2001).. Based on the transition probabilities, this is true for all regimes apart from the low inflation and low growth regime (top row in (45)). Furthermore, the system appears to never be in the low inflation and low growth regime as seen by the transition probabilities in the leftmost column.

$$\hat{A} = \{\hat{a}_{i,j}\} = \begin{bmatrix} 1.96e - 17 & 1.04e - 27 & 1.68e - 21 & 1.00e + 00 \\ 1.82e - 21 & 0.987 & 0.013 & 1.89e - 12 \\ 8.44e - 16 & 8.59e - 03 & 0.983 & 8.28e - 03 \\ 4.82e - 30 & 7.06e - 51 & 0.062 & 0.938 \end{bmatrix} \quad (45)$$

The estimated means for each regime $\hat{\mu}$, is shown in (46). With inflation in the left column and growth in the right. Based on the estimation of state means, we can label the states. From top to bottom, the state means are ordered as follows: low inflation with low growth (L,L), high inflation with high growth (H,H), low inflation with high growth (L,H), and high inflation with low growth (H,L).

$$\hat{\mu} = \begin{bmatrix} 0.00506342 & -0.01136599 \\ 0.02727511 & 0.05882335 \\ 0.01942035 & 0.03656246 \\ 0.05153785 & 0.02287326 \end{bmatrix} \quad (46)$$

The out-of-sample performance of the HMM (see Table 5), when fitted to the actual CPI and GDP data, is revealed to be more accurate in terms of RMSE relative to the random walk. A lower RMSE for the HMM compared to the random walk aligns with our simulation study, suggesting that the model performs well relative to the random walk when applied to real data. The results underline HMMs capability of adeptly mapping the dynamics of the financial markets consistent with Hua and Wang (2014); Nystrup et al. (2018); Çanakoglu and Özekici (2011). The enhanced predictive accuracy of the HMM during our out-of-sample period contradicts the findings of Dacco and Satchell (1999), which suggests that simple models such as random walk should yield better out-of-sample estimates than those of regime-switching models. The improved performance can be attributed to the random walk incurring significant penalties during regime shifts, resulting in higher RMSE values.

Table 5: HMM out-of-sample performance on CPI and GDP data

	RMSE CPI	RMSE GDP	AIC	Log Likelihood
Random Walk	0.0237	0.04517	-	-
HMM	0.0142	0.01409	-767.32	414.66

Figure 9 illustrates how the estimated probabilities for each state varies during the out-of-sample period. The line graphs shows the estimated probability of each state, at each point in time, corresponding to the value of the probability in the respective vertical axis. The first line graph with the headline *HMM Weights* shows estimates and consequently the dynamic weights used in portfolio construction produced by the HMM. The second line graph with the headline *HMM Weights with Exponential Moving Average* show the estimates and weights after smoothing the probabilities with exponential

weighted moving average, via the method presented in Section 3.4.5.

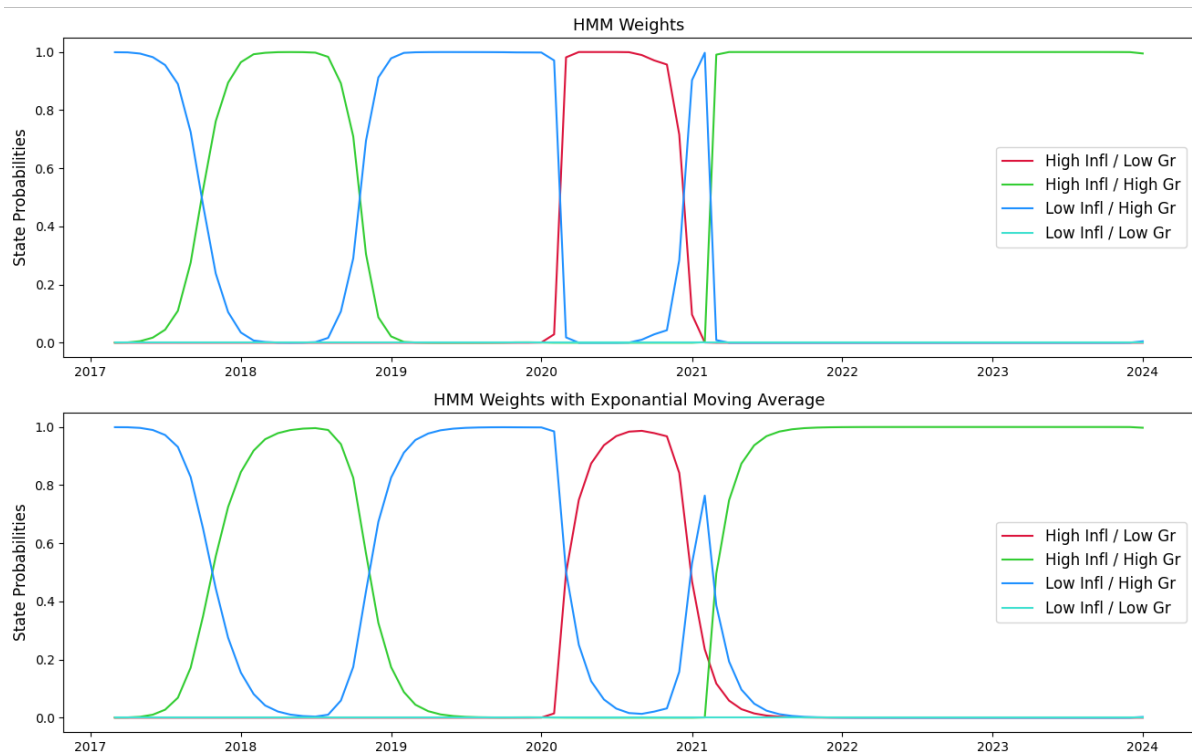


Figure 9: Probabilities for the four different market regimes over time, as predicted by the HMM. The first graph plots the HMM probabilities while the second plots the exponentially smoothed probabilities.

The two line graphs in Figure 9 indicate that the model estimates that each state will last for relatively long periods of six to twelve months. The sole deviation from this pattern is a brief period of low inflation and high growth towards the end of 2020 and the beginning of 2021.. We also note that the estimated probability for the low inflation and low growth state is constantly zero, which will result in no allocation towards this regimes state-optimal portfolio within any of the dynamic strategies.

As an estimated regime switch is approached, we initially notice how the current and upcoming state probabilities increase and decrease relative to each other at the same pace. By 2020 the estimated probabilities close to an estimated regime shift become more sharp and sudden, indicating a more volatile macroeconomic environment, which according to Liu (2011) should be beneficiary for a dynamic strategy. This increase in ambiguity of the macroeconomic environment is consistent with the behavior of the CPI and GDP when looking at the plotted values (see Figure 7) and coincides with the outbreak of the

pandemic.

Comparing the first and second line graphs without and with the exponential weighting moving average (EMA) the switches in the second line graph with the EMA are much smoother and more extended. This is an expected and intended effect of the exponential averaging of the HMM estimates.

6.2 Equal Weighted Portfolio Evaluation

Evaluating the static and dynamic portfolios that utilize the equally weighted method in any layer during the out-of-sample period March 1, 2017 - January 1, 2024, we see in Table 6, that the two dynamic HMM Equal Weighted portfolios perform better than the static portfolios in terms of total return, CAGR, and Sharpe ratio. The two portfolios HMM - EW and HMM - EW - EMA have a CAGR of 5.04% and 5.20%, respectively, which is higher than for any of the static portfolios. The static strategies are more stable as seen by the volatility; however, when looking at the Sharpe ratio, we see that the dynamic allocation generates higher returns relative to the risk. Better performance for the dynamic strategies is consistent with previous studies (Nystrup et al., 2018; Liu, 2011; Nguyen and Nguyen, 2015) and suggests that the state-dependent weighting manages to effectively calibrate its exposure to the prevailing market regime.

Table 6: Performance statistics for the equally weighted portfolios in the out of sample period.

	Total Return	CAGR	Volatility	Sharpe Ratio	Max Drawdown
Simple EW	22.43%	3.13%	7.07%	0.23	-16.38%
Layered EW	27.60%	4.39%	6.58%	0.41	-16.53%
HMM - EW	39.97%	5.04%	8.48%	0.42	-15.81%
HMM - EW - EMA	41.40%	5.20%	8.04%	0.46	-15.81%
S&P 500	98.41%	10.72%	17.69%	0.52	-34.30%

Shown in Figure 10, the dynamic and static portfolios generate a similar return for the approximate first four years of the sample period. However, by 2021 the dynamic portfolios diverge in an upward trajectory, indicating that the allocation effectively tilts the portfolio towards more favorable assets given the current market regime. The greater development

of the dynamic strategy continues for approximately two years, coinciding with the uptick in the stock market during the COVID pandemic. Thus, dynamic allocations can be assumed to effectively tilt the portfolio towards a more favorable exposure, aligning with previous findings (Kritzman et al., 2012; Nguyen and Nguyen, 2015; Kim et al., 2019). When comparing the development between the static and dynamic multi-asset portfolios to that of the S&P 500 we notice more stable but lesser returns during the sample period.

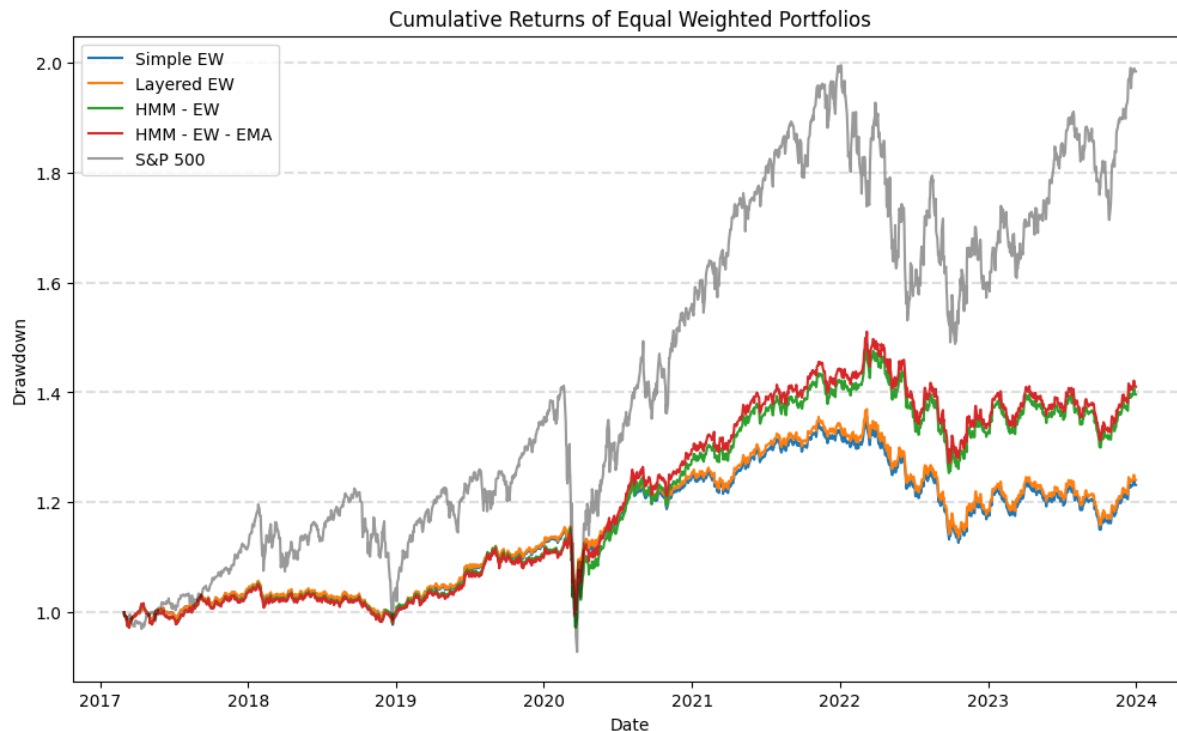


Figure 10: Cumulative returns for the equal weighted static and dynamic portfolios in the out-of-sample period.

The stability of the multi-asset portfolios is more evident when examining the declines in comparison to the S&P 500. Figure 11 illustrates the drawdowns from the cumulative maximum peak, at each point in time. Drawdowns for all the four EW-portfolios follow each other most of the time during the period. The two dynamic HMM portfolios have a slightly greater drawdown during the pandemic chock in 2020, compared to the static portfolios. However, from 2022 and forward, the two dynamic portfolios tend to have somewhat smaller drawdowns compared to the static ones. The higher resiliency of the dynamic portfolios towards the later part of the evaluation period suggests that the proactive allocation effectively manages downside risks during these market conditions (Nystrup et al., 2018). For the maximum drawdown for the whole period, there is hardly any

difference between the four portfolios with the Simple EW portfolio with the largest drawdown at -16.38% and the HMM - EW - EMA portfolio with the smallest drawdown at -15.8%. However, comparing these four portfolios with the S&P 500 during this period, the stock market tends to have greater drawdowns through the majority of the sample period. With the largest maximum drawdown at -34.30% for the S&P 500, the difference between the stock market and the four portfolios is greater, compared to the difference between the portfolios during the period.

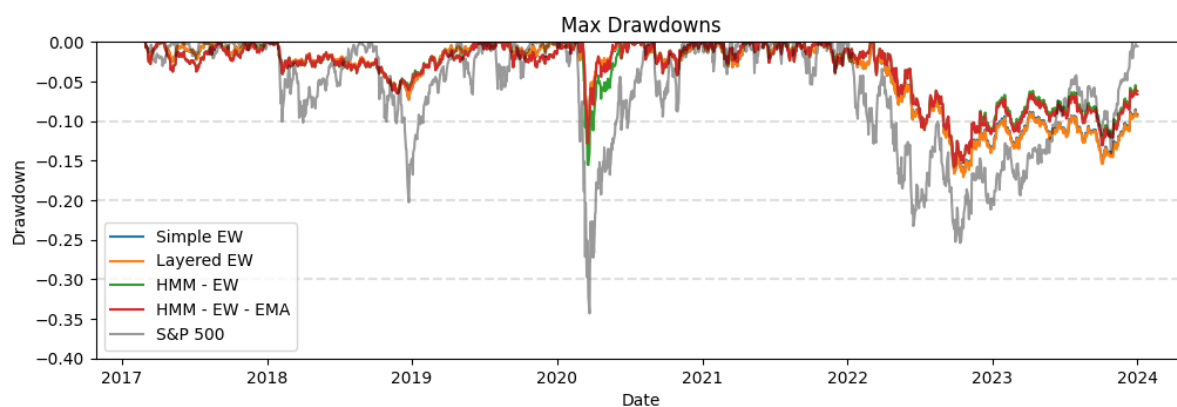


Figure 11: Drawdown of the equally weighed portfolios during the out-of-sample period.

Although neither of the static nor dynamic multi-asset portfolios manages to generate the same risk adjusted return as the S&P 500 it presents investor with an alternative during periods of downturn in equity markets due to its improved resiliency.

6.3 Risk Parity Portfolio Evaluation

This section evaluates the results and returns for the static and dynamic risk-parity portfolios during the out-of-sample period, March 1, 2017 - January 1, 2024.

Figure 12 and Table 7 shows results and returns for the four risk-parity portfolios and indicate that the two dynamic portfolios perform better compared to the static portfolios in terms of total return, CAGR and Sharpe ratio. During the evaluation period, the dynamic portfolios HMM - RP and HMM - RP - EW had a significantly higher total return compared to the static risk-parity portfolios, once again suggesting the ability of a dynamic investment strategy to deliver superior performance relative to traditional and static strategies, as proposed by Elliott and Hinz (2002); Nystrup et al. (2018); Liu (2011) among others. The same is true when comparing the four CAGRs: HMM - RP and HMM

- RP - EMA have a CAGR of 6.34% and 6.67% respectively, compared to the CAGRs of 2.16% and 2.73% for Simple RP and Layered RP respectively. When looking at return relative to the risk we observe the largest Sharpe ratio for the dynamic portfolios at 0.58 and 0.64.

During the out-of-sample period, the two dynamic HMM portfolios have a higher volatility compared to the simple and layered portfolios. However, comparing the respective EW and RP counterpart portfolios in pairs, three of four risk-parity portfolios show lower volatility compared to their equal weighted counterparts. Only HMM - RP - EMA has a higher volatility compared to its counterpart HMM - EW - EMA. Despite the higher volatility, HMM - RP - EMA still shows a higher Sharpe ratio at 0.64, compared to its counterpart HMM - EW - EMA with a Sharpe ratio at 0.46. This is true for the non-smoothed dynamic portfolios as well, where HMM - RP has a higher Sharpe Ratio compared to HMM - EW, while the opposite is true for the static portfolios. This indicates that applying dynamic weights within the risk-parity framework results in higher potential gains and more effectively adjusts allocations towards assets with better returns.

Table 7: Performance statistics for the risk-parity portfolios during the out-of-sample period.

	Total Return	CAGR	Volatility	Sharpe Ratio	Max Drawdown
Simple RP	15.47%	2.16%	6.59%	0.10	-19.04%
Layered RP	20.22%	2.73%	7.11%	0.17	-16.28%
HMM - RP	52.16%	6.34%	8.39%	0.58	-12.71%
HMM - RP - EMA	55.42%	6.67%	8.14%	0.64	-12.80%
S&P 500	98.41%	10.72%	17.69%	0.52	-34.30%

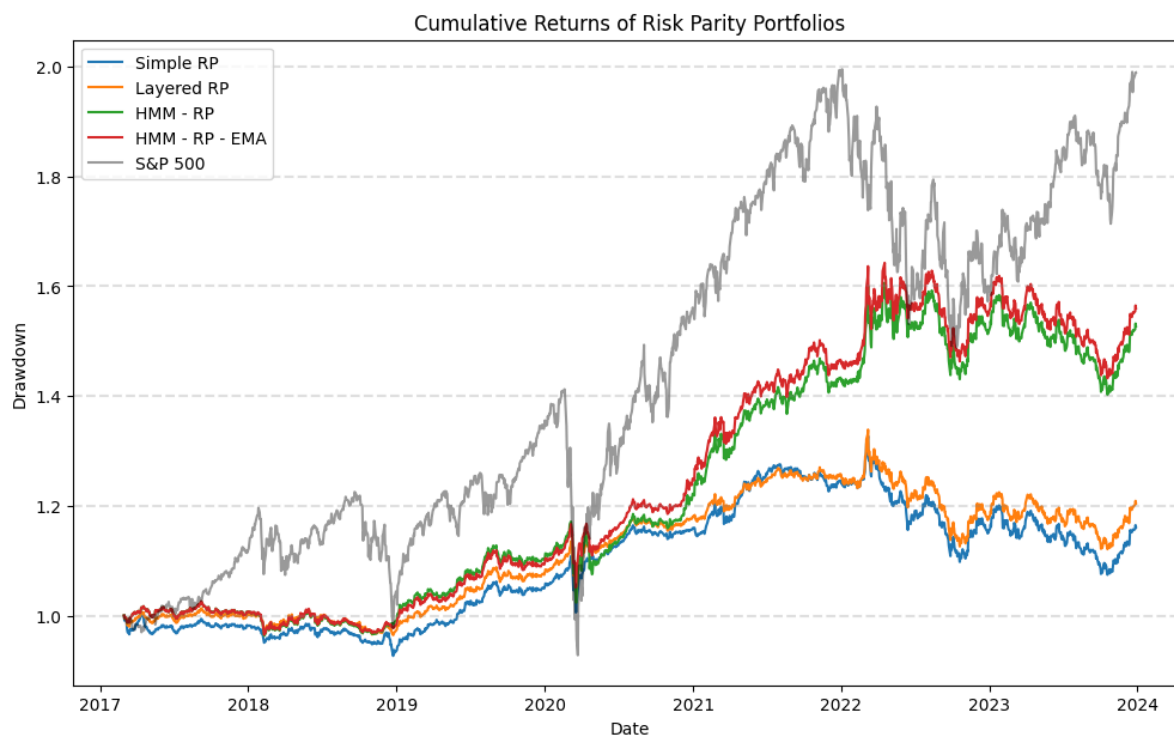


Figure 12: Cumulative returns for the risk parity portfolios during the out-of-sample period.

Figure 13 shows the drawdowns from the cumulative maximum peak at each point in time during the full evaluation period. Unlike the EW-portfolios, there is some difference in the drawdowns between the RP-portfolios. Generally, the two HMM portfolios tend to have slightly smaller drawdowns for the entire out-of-sample period. Around the pandemic-check in 2020, the two HMM portfolios, once again, have bigger drawdowns. However, from 2022 and forward, the two HMM portfolios show greater resilience with smaller drawdowns compared to the static portfolios. These differences are the greatest deviations during the period. Compared to the S&P 500, it is evident that drawdowns occur approximately at the same times, but the troughs of the equity market are significantly deeper. Looking at the maximum drawdowns for the whole period in Table 7, there is a very big difference between the Simple RP portfolio with the largest maximum drawdown at -19.04% and the HMM - RP portfolio with the smallest maximum drawdown at -12.80%. This difference becomes even greater compared to the maximum drawdown of the S&P 500 which once again is -34.30% during this period. Deeper troughs for the equity market are in line with the intended purpose of the risk parity weighting method due to its inherent aim of providing more stable and resilient returns over time (Bridgewater, 2012; Qian, 2011; Prince, 2010).

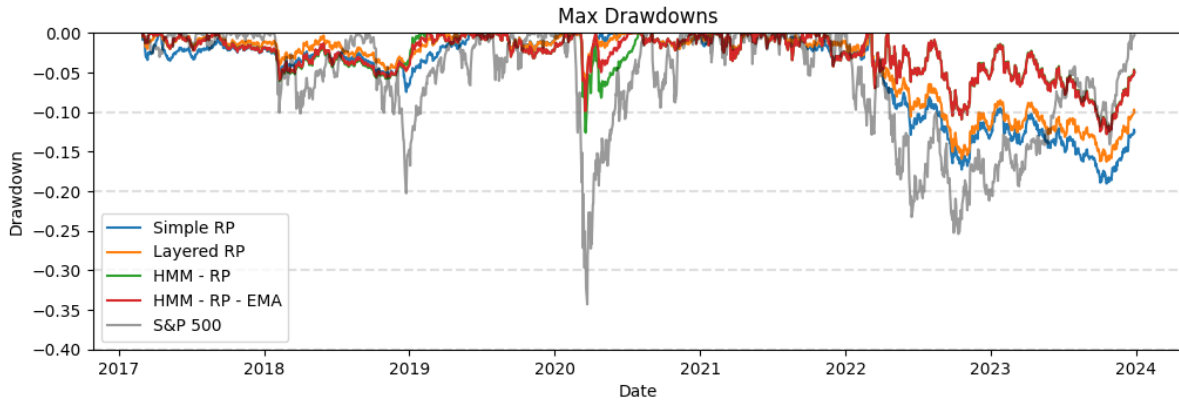


Figure 13: Drawdown for the risk parity portfolios during the out-of-sample period.

When comparing the equal-weighted and risk-parity portfolios in pairs, three of four risk-parity portfolios have a smaller maximum drawdown, compared to their equal-weighted counterpart. Only the Simple RP portfolio has a greater maximum drawdown, compared to the Simple EW portfolio. In general, these findings align with the conclusions made by Bessler et al. (2021), which stated that risk parity can improve portfolio resilience. However, in this study, the claims of Prince (2010) and Qian (2011) that risk-parity would offer a more consistent performance across market dynamics fluctuations relative to traditional allocation strategies cannot be confirmed.

A possible explanation for the underwhelming performance of the layered static risk-parity portfolio is the overlap for each sub-portfolio. As mentioned earlier, the portfolio constructions of this study, regarding the optimal asset classes in each sub-portfolio, are based on previous findings and recommendations. One of the critical aspects when building a risk parity portfolio, as pointed out by Fabozzi et al. (2021), is the selection of assets. When studying the behavior of each sub-portfolio during the out-of-sample period, it becomes apparent that they are highly correlated and thus offer limited diversification possibilities. The high correlation stems from an overlap in each portfolio's assets. By conducting a robust study on the selection of optimal assets during each market regime, the framework proposed in this study could potentially be developed into a more robust and profitable investment strategy.

6.4 Transaction Costs

When transaction costs are factored into each portfolio, there is a significant drop in performance for all risk-parity portfolios. The equally weighted portfolios also experience a decline in returns and Sharpe ratios, though the impact is less severe. This is explained by the volatile asset allocation within each risk-parity portfolio relative to the very stable allocation in the equally weighted portfolios.

The smoothed HMM portfolios are after transaction cost the portfolios with the highest total return and Sharpe ratio; however, in contrast to the results without transaction cost, the equally weighted portfolios are now outperforming their risk-parity counterpart. We observe that the dynamic strategy still performs better than the static in all terms except volatility, which is consistent with previous findings suggesting that dynamic asset allocation provides better performance (Nguyen and Nguyen, 2015; Nystrup et al., 2018; Liu, 2011). The better performance indicates that the dynamic allocation successfully shifts the portfolio towards the appropriate assets, implying that our HMM model adeptly adjusts the weights to benefit the portfolio. This underlies the viability of using HMM as an input in creating a state-dependent portfolio allocation as previous studies have suggested (Nguyen and Nguyen, 2015; Nystrup et al., 2018; Kritzman et al., 2012; Liu, 2011).

Table 8: Performance statistics when accounting for transaction costs in all portfolios during the full out-of-sample period.

	Total Return	CAGR	Volatility	Sharpe Ratio	Max Drawdown
EW	21.72%	2.96%	7.07%	0.21	-17.08%
RP	4.75%	0.69%	6.61%	-0.12	-20.93%
EW EW	32.43%	4.26%	7.10%	0.39	-16.66%
RP RP	9.04%	1.29%	6.33%	-0.03	-17.62%
HMM EW	36.67%	4.75%	8.48%	0.38	-15.94%
HMM RP	34.25%	4.47%	8.49%	0.35	-14.46%
HMM EW EMA	38.12%	4.92%	8.04%	0.43	-15.94%
HMM RP EMA	37.17%	4.81%	8.24%	0.40	-14.35%

The drops in the portfolio performances when adding transaction costs to the monthly re-balancing, advocates for future research that search for the optimal re-balancing frequency, taking the transaction costs in consideration. This is a part that has been left out in this study due to limitations. Also, comparing different weighting methods beyond the equal weighted and risk-parity approach in combination with the HMM weighing is an area that warrants further exploration.

6.5 Factor Performance Analysis

The daily returns of the strategy without transaction costs are further evaluated against a factor model, namely the Fama-French five factors expanded to include the momentum factor. The only portfolio that manages to generate a significantly positive alpha value is the dynamic risk-parity strategy with smoothed weights. The HMM - RP - EMA produces a positive daily alpha of 0.0002 with significance at 90%. However, even if none of the remaining portfolios is able to produce significantly positive alpha values, the factor model presents interesting results in terms of how the portfolios are correlated to the equity market. All static and dynamic portfolios have significant beta coefficients for the excess market return at 99%. The low beta coefficients for excess returns imply that these portfolios could provide utility in hedging against volatility in the equity market. The portfolio with the highest beta coefficient towards the market is the HMM - EW portfolio, where the lowest is found in the layered risk-parity portfolio. The fact that the layered risk-parity portfolio is least correlated towards the market is expected due to the equity index being the second riskiest asset out of the seven and thus constitutes a small part of the total portfolio allocation. In fact, all risk parity portfolios exhibit a lower beta coefficient compared to their equally weighted counterparts, further highlighting their effectiveness in reducing the dependence on the stock market as intended (Bridgewater, 2009; Qian, 2011; Prince, 2010). A further examination of the other factors is unnecessary given the portfolio structure. Since all portfolios have limited exposure to equities, evaluating the other factors in relation to performance would not provide further insights.

Table 9: Portfolio regression on the daily returns against daily Fama-French six factors. Reported in parenthesis is heteroskedasticity-consistent standard errors. (Significance Levels: * = 90%, ** = 95%, *** = 99%)

	α	Mkt-RF	SMB	HML	RSW	CMA	WML
Simple EW	-0.0001	0.1742***	0.0337	-0.0468*	-0.0419*	0.0873*	-0.0028
	(7.27e-05)	(0.012)	(0.021)	(0.025)	(0.025)	(0.036)	(0.013)
Simple RP	-1.393e-05	0.0846***	0.0498*	-0.0637**	-0.0690**	0.0908**	-0.0006
	(9.6e-05)	(0.014)	(0.026)	(0.029)	(0.031)	(0.045)	(0.015)
Layered EW	5.887e-05	0.1869***	0.0450**	-0.0677**	-0.0501*	0.1101**	0.0142
	(8.26e-05)	(0.013)	(0.023)	(0.027)	(0.026)	(0.040)	(0.013)
Layered RP	4.996e-05	0.0784***	0.0400*	-0.0690***	-0.0851***	0.1102***	0.0005
	(8.23e-05)	(0.008)	(0.016)	(0.018)	(0.022)	(0.029)	(0.009)
HMM - EW	0.0009	0.2692***	0.0248	-0.0230	-0.1257***	0.1356**	0.0235
	(0.000)	(0.016)	(0.026)	(0.031)	(0.030)	(0.043)	(0.015)
HMM - RP	0.0002	0.1436***	0.0315	-0.0543	-0.1982***	0.1799***	0.0180
	(0.000)	(0.018)	(0.035)	(0.036)	(0.047)	(0.056)	(0.017)
HMM - EW - EMA	7.562e-05	0.2191***	0.0433	-0.0391	-0.1264***	0.1148**	0.0173
	(0.000)	(0.016)	(0.027)	(0.031)	(0.032)	(0.046)	(0.016)
HMM - RP - EMA	0.0002*	0.1170***	0.0366	-0.0647*	-0.2073***	0.1711**	0.0138
	(0.000)	(0.018)	(0.031)	(0.034)	(0.046)	(0.056)	(0.017)

7 Conclusions

This paper has explored the integration of Hidden Markov Models (HMM) with risk-parity and equally weighted portfolios to create a dynamic state-dependent allocation. The integration offers a promising approach for navigating different market regimes and adjusting portfolio allocation based on macroeconomic conditions. The dynamic strategy demonstrates significant improvements, including higher risk adjusted returns and reduced drawdowns in out-of-sample evaluation relative to static risk-parity and equal weighted strategies. The empirical results highlight the effectiveness of incorporating the state probabilities estimated by HMMs to enhance portfolio resilience and optimize asset allocation to varying macroeconomic environments. Despite challenges for the HMM in accurately predicting short-term regime shifts, the model's ability to adapt to longer regimes contributes to the overall robustness and usage of dynamic investment strategies. Additionally, the use of HMM allows for a more detailed understanding of the market's underlying states, enabling more precise adjustments to portfolio allocations (Hua and Wang, 2014; Çanakoglu and Özekici, 2011). This adaptivity is particularly valuable in volatile market environments, such as today, where traditional models may fall short (Liu, 2011). The successful application of HMM in out-of-sample forecasting of CPI and GDP, relative to a simple random walk model, is contrary to Dacco and Satchell (1999) critique regarding the unreliable out-of-sample performance of regime-switching models. Extending the dynamic strategy using additional macroeconomic indicators that have been shown to affect asset performance such as those shown by Ang and Chen (2002); Huang et al. (2016), could provide additional upside to the dynamic strategy. Moreover, this study contributes to the broader financial literature by further demonstrating how statistical methods, such as the HMM, can be used to manage portfolio risk and improve returns.

Further research could focus on the interaction between asset return and economic climate in the context of market regimes to provide a more solid optimization for each sub-portfolio. The continued development of dynamic investment strategies can provide investors with a more robust framework for more stable and resilient returns, especially during periods of economic ambiguity. The insights in this paper align with previous studies by Kritzman et al. (2012); Nguyen and Nguyen (2015), to name a few, on the

usage of data-driven investment strategies to boost portfolio performance.

In general, dynamic portfolio construction using HMM and risk parity offers a greater potential for portfolio improvement than the usage of an equally weighted dynamic strategy. However, due to the complexity of the model and real-world complications, such as transaction costs, a direct practical implementation of this exact strategy might be limited.

References

- Akaike, H. (1974). A new look at the statistical model identification. *IEEE transactions on automatic control*, 19(6):716–723.
- Aleksandar Andonov, F. B. and Lehnert, T. (2010). Tips, inflation expectations, and the financial crisis. *Financial Analysts Journal*, 66(6):27–39.
- Ang, A. and Chen, J. (2002). Asymmetric correlations of equity portfolios. *Journal of Financial Economics*, 63(3):443–494.
- Baker, J. (1975). The dragon system—an overview. *IEEE TRANS.ACOUST.SPEECH SIG.PROC*, 23(1):24–29.
- Baum, L. E. (1968). Growth functions for transformations on manifolds. *Pac. J. Math.*, 27(2):211–227.
- Bessler, W., Taushanov, G., and Wolff, D. (2021). Factor investing and asset allocation strategies: a comparison of factor versus sector optimization. *Journal of asset management*, 22(6):488–506.
- Bouchev, P., Nemtchinov, V., Paulsen, A., and Stein, D. M. (2012). Volatility harvesting: Why does diversifying and rebalancing create portfolio growth? *Journal of Wealth Management*, 15(2):26–35.
- Bridgewater (2009). The All Weather Strategy. https://sdcera.granicus.com/MetaViewer.php?view_id=4&clip_id=75&meta_id=9141. Accessed: 10.02.2024.
- Bridgewater (2012). The All Weather Story. https://www.bridgewater.com/_document/the-all-weather-story?id=00000171-8623-d7de-affd-feaf4ee20000. Accessed: 07.01.2024.
- Cappiello, L., Engle, R. F., and Sheppard, K. (2006). Asymmetric dynamics in the correlations of global equity and bond returns. *Journal of Financial Econometrics*, 4(4):537–572.
- Chua, D. B., Kritzman, M., and Page, S. (2009). The myth of diversification. *Journal of Portfolio Management*, 36(1):26–35.
- Chung Baek, T. J. (2021). Safe-haven assets for u.s. equities during the 2020 covid-19 bear market. *Economics and Business Letters*, 10:331–335.
- Council On Foreign Relations (2012). A conversation with ray dalio. <https://www.youtube.com/watch?v=SFaRazMpxcM&t=8s>. Accessed: 07.01.2024.
- Dacco, R. and Satchell, S. (1999). Why do regime-switching models forecast so badly? *Journal of Forecasting*, 18(1):1–16.
- Dahlquist, M. and Harvey, C. R. (2001). Global tactical asset allocation. *Available at SSRN 795376*.
- DeMiguel, V., Garlappi, L., and Uppal, R. (2009). Optimal versus naive diversification: How inefficient is the 1/n portfolio strategy? *Review of Financial studies*, 22(5):1915–1953.

- Elliott, R. and Hinz, J. (2002). Portfolio optimization, hidden markov models and technical analysis of p&f charts. *International Journal of Theoretical and Applied Finance*, 5:385–399.
- Fabozzi, F. A., Simonian, J., and Fabozzi, F. J. (2021). Risk parity: The democratization of risk in asset allocation. *The Journal of Portfolio Management*, 47(5):41–50.
- Fisher, G. S., Maymin, P. Z., and Maymin, Z. G. (2015). Risk parity optimality. *Journal of Portfolio Management*, 41(2):42.
- Flannery, M. J. and Protopapadakis, A. A. (2002). Macroeconomic factors do influence aggregate stock returns. *Review of Financial Studies*, 15(3):751–782.
- Forney, G. (1973). The viterbi algorithm. *Proceedings of the IEEE*, 61(3):268–278.
- Fuertes Mendoza, A. (2023). The effectiveness of different asset types as a hedge against inflation. *Economic Bulletin*, (2023/Q1):03.
- Glasserman, P. and Merener, N. (2003). Cap and swaption approximations in libor market models with jumps. *Journal of Computational Finance*, 7(1):1–36.
- Grossman, S. J. and Zhou, Z. (1993). Optimal investment strategies for controlling drawdowns. *Mathematical finance*, 3(3):241–276.
- Hua, Y. and Wang, X. (2014). Portfolio selection with a hidden markov model. *Quality Technology & Quantitative Management*, 11:167–174.
- Huang, W., Mollick, A. V., and Nguyen, K. H. (2016). U.s. stock markets and the role of real interest rates. *The Quarterly Review of Economics and Finance*, 59:231–242.
- Juang, B.-H. (1985). Maximum-likelihood estimation for mixture multivariate stochastic observations of markov chains. *AT&T technical journal*, 64(6):1235–1249.
- Juang, B.-H., Levinson, S., and Sondhi, M. (1986). Maximum likelihood estimation for multivariate mixture observations of markov chains (corresp.). *IEEE Transactions on Information Theory*, 32(2):307–309.
- Kim, E.-c., Jeong, H., and Lee, N.-y. (2019). Global asset allocation strategy using a hidden markov model. *Journal of Risk and Financial Management*, 12(4):168.
- Kritzman, M., Page, S., and Turkington, D. (2012). Regime shifts: Implications for dynamic strategies (corrected). *Financial Analysts Journal*, 68(3):22–39.
- Laatsch, F. E. and Klein, D. P. (2003). Nominal rates, real rates, and expected inflation: Results from a study of u.s. treasury inflation-protected securities. *Quarterly Review of Economics and Finance*, 43(3):405–417.
- Leal, R. P. C. and de Melo Mendes, B. V. (2005). Maximum drawdown: Models and applications. *The Journal of Alternative Investments*, 7(4):83–91.
- Liporace, L. (1982). Maximum likelihood estimation for multivariate observations of markov sources. *IEEE transactions on information theory*, 28(5):729–734.

- Liu, H. (2011). Dynamic portfolio choice under ambiguity and regime switching mean returns. *Journal of Economic Dynamics and Control*, 35(4):623–640.
- Magnus Andersson, E. K. and Vähämaa, S. (2008). Why does the correlation between stock and bond returns vary over time? *Applied Financial Economics*, 18(2):139–151.
- Masoud, N. M. (2013). The impact of stock market performance upon economic growth. *International Journal of Economics and Financial Issues*, 3(4):788–798.
- Messina, E. and Toscani, D. (2008). Hidden markov models for scenario generation. *IMA Journal of Management Mathematics*, 19(4):379–401.
- Nguyen, N. (2018). Hidden markov model for stock trading. *International Journal of Financial Studies*, 6(2):36.
- Nguyen, N. and Nguyen, D. (2015). Hidden markov model for stock selection. *Risks*, 3(4):455–473.
- Novak, D. G. et al. (2022). *The fama and french six-factor model: evidence for the german market*. PhD thesis.
- Nystrup, P., Madsen, H., and Lindström, E. (2018). Dynamic portfolio optimization across hidden market regimes. *Quantitative Finance*, 18(1):83–95.
- Plyakha, Y., Uppal, R., and Vilkov, G. (2012). Why does an equal-weighted portfolio outperform value-and price-weighted portfolios? Available at SSRN 2724535.
- Prince, B. (2010). Risk parity is about balance. <https://www.pionline.com/assets/docs/CO760371018.PDF>. Accessed: 10.02.2024.
- Psaradakis, Z. and Spagnolo, N. (2003). On the determination of the number of regimes in markov-switching autoregressive models. *Journal of time series analysis*, 24(2):237–252.
- Qian, E. (2011). Risk parity and diversification. *Journal of Investing*, 20(1):119.
- Rabiner, L. R. (1989). A tutorial on hidden markov models and selected applications in speech recognition. *Proceedings of the IEEE*, 77(2):257–286.
- Reuters (2022). How 2022 shocked, rocked and rolled global markets. <https://www.reuters.com/markets/global-markets-wrapup-1-pix-2022-12-22/>. Accessed: 2024-04-24.
- Robles, B., Avila, M., Duculty, F., Vrignat, P., Begot, S., and Kratz, F. (2012). Methods to choose the best hidden markov model topology for improving maintenance policy. In *9th International Conference on Modeling, Optimization & SIMulation*.
- Roman, D., Mitra, G., and Spagnolo, N. (2010). Hidden markov models for financial optimization problems. *IMA Journal of Management Mathematics*, 21(2):111–129.
- Roncalli, T. (2013). *Introduction to risk parity and budgeting*. CRC Press.
- Shahidi, A. and Lee, B. (2014). *Balanced Asset Allocation: How to Profit in Any Economic Climate*. Wiley finance. Wiley, Newark, 1st edition.

-
- Viterbi, A. (1967). Error bounds for convolutional codes and an asymptotically optimum decoding algorithm. *IEEE transactions on Information Theory*, 13(2):260–269.
- Çanakoglu, E. and Özekici, S. (2011). Portfolio selection with imperfect information: A hidden markov model. *Applied Stochastic Models in Business and Industry*, 27:95–114.

Appendix

A ETF Factor Regression

Table 10: Regression on the daily returns of each ETF against daily Fama-French six factors. Reported in parenthesis is heteroskedasticity-consistent standard errors. (Significance Levels: * = 90%, ** = 95%, *** = 99%)

	alpha	MktRf	SMB	HML	RMW	CMA	WML
DBC	-0.0049*** (0.000)	0.4310*** (0.035)	0.0605 (0.061)	0.3161*** (0.071)	-0.4734*** (0.080)	0.2293** (0.114)	0.1192*** (0.035)
GLD	-0.0048*** (0.000)	0.0650* (0.035)	0.1395** (0.059)	-0.2150*** (0.060)	-0.1586** (0.068)	0.4490*** (0.092)	0.0852** (0.035)
IEI	-0.0052*** (0.000)	-0.0338*** (0.013)	0.0628** (0.030)	-0.0862** (0.035)	0.0342 (0.040)	0.0942 (0.058)	-0.0184 (0.017)
TIP	-0.0052*** (0.000)	0.0109 (0.022)	0.0921** (0.037)	-0.0619 (0.044)	-0.0026 (0.046)	0.0792 (0.074)	7.695e-05 (0.019)
TLT	-0.0051*** (0.000)	-0.2165*** (0.039)	0.1850*** (0.069)	-0.3138*** (0.075)	0.1169 (0.075)	0.1102 (0.117)	-0.0114 (0.037)
VCIT	-0.0052*** (0.000)	0.0781*** (0.024)	0.0942* (0.053)	-0.0804 (0.051)	0.0829* (0.047)	0.0738 (0.073)	-0.0205 (0.022)
VOO	-0.0052*** (0.000)	1.0069*** (0.012)	-0.1253*** (0.030)	-8.823e-05 (0.033)	0.0546 (0.037)	0.1117** (0.054)	-0.0067 (0.015)

B Returns and drawdowns adjusted for transaction costs

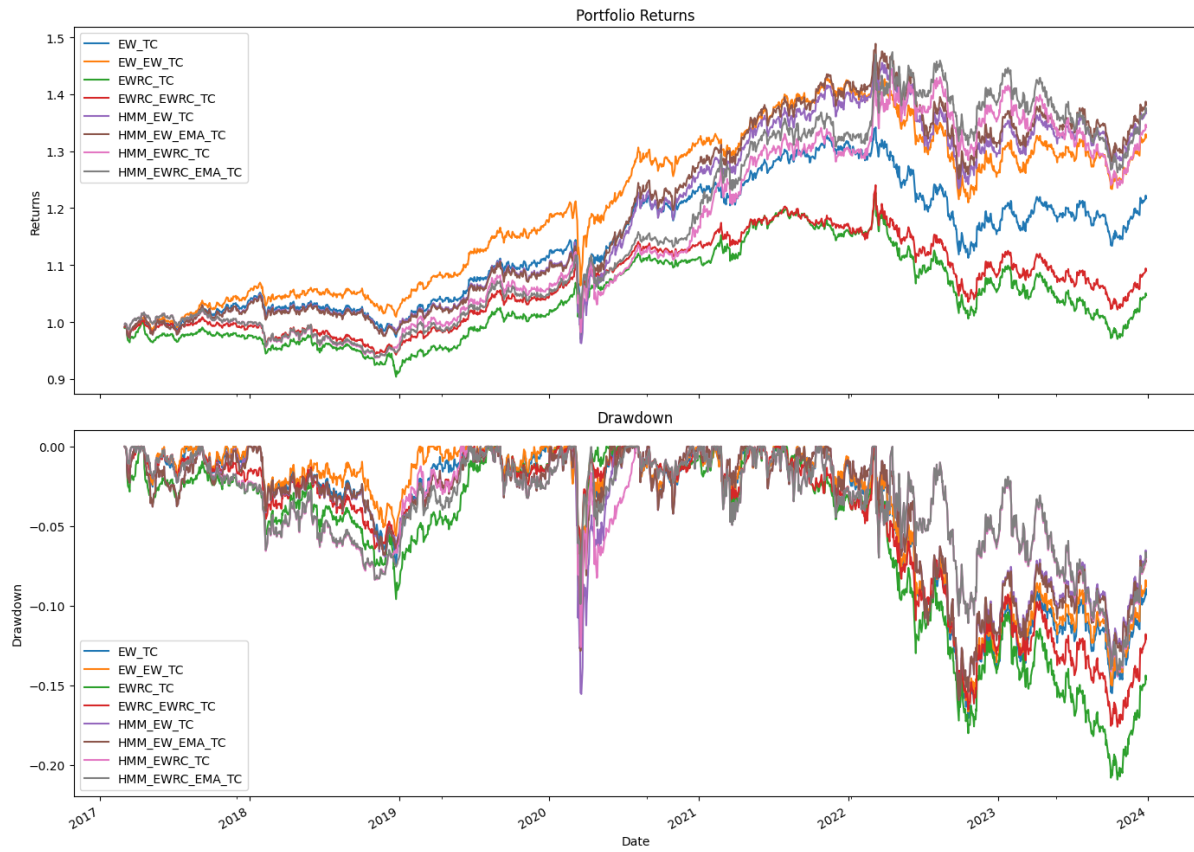


Figure 14: Cumulative returns and drawdowns for each portfolio accounting for transaction costs during the full out-of-sample period.